This is a post-peer-review, pre-copyedit version of an article published in Journal of the American Society for Mass Spectrometry. The final authenticated version is available online at: https://doi.org/10.1007/s13361-019-02346-9

This version is available from https://hdl.handle.net/10195/75021

This postprint version is licenced under a Creative Commons Attribution-NonCommercial-NoDerivatives 4.0.International.

Journal of The American Society for Mass Spectrometry

Comparison of clusters produced from Sb2Se3 homemade polycrystalline material, thin films and commercial polycrystalline bulk using laser desorption ionisation with time of flight quadrupole ion trap mass spectrometry

--Manuscript Draft--

Manuscript Number:	ASMS-D-19-00224R1
Full Title:	Comparison of clusters produced from Sb2Se3 homemade polycrystalline material, thin films and commercial polycrystalline bulk using laser desorption ionisation with time of flight quadrupole ion trap mass spectrometry
Short Title:	Clusters from various Sb2Se3 materials
Article Type:	Original Article
Keywords:	antimony selenide; clusters; laser desorption ionisation; paraffin; chalcogenides
Corresponding Author:	Josef Havel Masaryk University Brno, CZECH REPUBLIC
Corresponding Author Secondary Information:	
Corresponding Author's Institution:	Masaryk University
Corresponding Author's Secondary Institution:	
First Author:	Fei Huang, Mgr
First Author Secondary Information:	
Order of Authors:	Fei Huang, Mgr
	Lubomír Prokeš, PhD
	Petr Němec, PhD
	Virginie Nazabal, Prof
	Josef Havel
Order of Authors Secondary Information:	
Funding Information:	Grantová Agentura České Republiky (Projects No. 18-03823S) — Dr. Josef Havel
Abstract:	Abstract. This study compared Sb2Se3 material in the form of commercial polycrystalline bulk, sputtered thin film and homemade polycrystalline material using laser desorption ionisation (LDI) time of flight mass spectrometry with quadrupole ion trap mass spectrometry. It also analysed the stoichiometry of the SbmSen clusters formed. The results showed that homemade Sb2Se3 bulk was more stable compared to thin film; its mass spectra showed the expected cluster formation. The use of materials for surface-assisted LDI (SALDI), i.e., graphene, graphene oxide and C60, significantly increased the mass spectra intensity. In total, nineteen SbmSen clusters were observed. Six novel, high-mass clusters—Sb4Se4+, Sb5Se3-6+ and Sb7Se4+—were observed for the first time when using paraffin as a protective agent.

Powered by Editorial Manager® and ProduXion Manager® from Aries Systems Corporation

Manuscript clean

Click here to view linked References

Comparison of clusters produced from Sb_2Se_3 homemade polycrystalline material, thin films and commercial polycrystalline bulk using laser desorption ionisation with time of flight quadrupole ion trap mass spectrometry

Fei Huang,[1] Lubomír Prokeš,[1] Petr Němec,[2] Virginie Nazabal,[2,3] and Josef Havel[1*]

[1]Department of Chemistry, Faculty of Science, Masaryk University, Kamenice 5/A14, 62500 Brno, Czech Republic

[2]Department of Graphic Arts and Photophysics, Faculty of Chemical Technology, University of Pardubice, Studentská 573, 53210 Pardubice, Czech Republic

[3]Institut des Sciences Chimiques de Rennes, UMR-CNRS 6226, Equipe Verres et Céramiques, Université de Rennes 1, 35042 Rennes, France

*Author to whom correspondence should be addressed. Email: havel@chemi.muni.cz

Phone: +420 549494114, Fax: +420 549492494

Abstract. This study compared Sb_2Se_3 material in the form of commercial polycrystalline bulk, sputtered thin film and homemade polycrystalline material using laser desorption ionisation (LDI) time of flight mass spectrometry with quadrupole ion trap mass spectrometry. It also analysed the stoichiometry of the Sb_mSe_n clusters formed. The results showed that homemade Sb_2Se_3 bulk was more stable compared to thin film; its mass spectra showed the expected cluster formation. The use of materials for surface-assisted LDI (SALDI), i.e., graphene, graphene oxide and C_{60}, significantly increased the mass spectra intensity. In total, nineteen Sb_mSe_n clusters were observed. Six novel, high-mass clusters—$Sb_4Se_4^+$, $Sb_5Se_{3-6}^+$ and $Sb_7Se_4^+$—were observed for the first time when using paraffin as a protective agent.

Keywords: antimony selenide; clusters; laser desorption ionisation; paraffin; chalcogenides

Introduction

Sb_2Se_3, which is known in nature as the mineral antimonselite. The crystal and electronic structure of antimony selenide as well as its vibrational properties were previously determined [1-4]. Generally, the Sb_mSe_n system is an important member of chalcogenide materials. Under typical experimental conditions of chalcogenide glass synthesis, the glass-forming region in the Sb_mSe_n system is limited to rather low antimony content (up to 30%), and smaller glass batches often face phase separation problems [5-7]. On the other hand, it is possible to fabricate amorphous,

stoichiometric and thin Sb_2Se_3 films by physical vapour deposition techniques such as radio-frequency magnetron sputtering [8] or thermal evaporation [9]. Moreover, Sb_2Se_3 forms stable glasses and amorphous thin films with other glass-forming selenides like $GeSe_2$ [10-13]. Today, Sb_mSe_n materials, especially in the form of thin films, have been widely studied as amorphous thin films of Sb_2Se_3 for memory switching application [14-15], as glass-ceramic or antimony selenide thin films for solar cells [16-20], as Sb_2Se_3 anode for lithium, and sodium batteries [21-22].

In a previous article [23], we examined the formation of clusters produced by laser ablation from mixtures of Sb and Se elements in different ratios. We observed 24 Sb_mSe_n clusters that were generated from metal surface of common target. In this study, we would like to compare the stoichiometry of clusters formed by laser desorption ionisation (LDI) from Sb_2Se_3 materials in the form of commercial polycrystalline bulk, thin film, and homemade polycrystalline material to the clusters generated by laser ablation synthesis (LAS) from the mixtures of elements (antimony and selenium). Additionally, in order to evaluate the influence of various surfaces on cluster formation, some other materials that act as surface-assisted LDI (SALDI) matrices (graphene [G], graphene oxide [GO] and fullerene [C_{60}]) were used. Since paraffin (as a protective agent) was found to increase the intensity of chalcogenide high mass clusters [24], we also studied the assistance of paraffin in detail.

Experimental

Chemicals

Polycrystalline Sb_2Se_3 was purchased from Sigma-Aldrich (St. Louis, MO, USA). Homemade polycrystalline Sb_2Se_3 was synthesised using high-purity elements (Sb and Se of 99.999% purity). Acetonitrile, G, GO and C_{60} were purchased from Sigma-Aldrich (Steinheim, Germany). Parafilm was purchased from Bemis NA (Neenah, Wis., USA). Red phosphorus was obtained from Riedel de Haën (Hannover, Germany) and was purified via sublimation in a nitrogen atmosphere. Water was double distilled using a quartz apparatus from Heraeus Quarzschmelze (Hanau, Germany). All other reagents were of analytical-grade purity. Amorphous Sb_2Se_3 thin films were fabricated by radio-frequency magnetron sputtering using an MPE600S (Plassys-Bestek, France) multichamber physical vapour deposition system. For the depositions, single crystalline silicon <100> substrates and a polycrystalline Sb_2Se_3 sputtering target (99.999%, ALB Materials, USA) were employed. The experimental details of thin film deposition are provided elsewhere [8]. No Bragg peaks were detected in the X-ray diffraction patterns of deposited thin films, data that confirm their amorphous state.

Mass spectrometry

AXIMA Resonance and AXIMA CFR mass spectrometers, both from Kratos Analytical Ltd. (Manchester, UK), coupled with a quadrupole ion trap and time-of-flight detection, were used to record mass spectra in both positive and negative ion modes. Both instruments were equipped with a nitrogen laser (337 nm), and the laser repetition rate was set to 5 Hz with a pulse time width of 3 ns.

Software and computation

Launchpad software (Kompact version 2.9.3, 2011) from Kratos Analytical Ltd. (Manchester, UK) was used to determine Sb_mSe_n cluster stoichiometry via comparison of isotopic envelopes.

Sample preparation for mass spectrometry

1. Commercial Sb_2Se_3 polycrystalline bulk, homemade polycrystalline material and amorphous Sb_2Se_3 thin film

An agate mortar was used to pulverise the polycrystalline Sb_2Se_3; the powder was then suspended in acetonitrile (1 mg/ml). From the prepared suspensions, 10 µL was deposited on a MALDI target and dried in open air. The amorphous Sb_2Se_3 thin film was fixed on the target with a narrow piece of parafilm.

2. SALDI using GO, G and C_{60} surfaces

Ten µL of GO, G, or C_{60} suspensions in acetonitrile were separately deposited on individual spots of a MALDI target, and then 10 µL of the commercial polycrystalline bulk Sb_2Se_3 powder suspension (described above) was separately added on the surface of the GO, G or C_{60} suspension.

3. Sb_2Se_3 covered with paraffin

Ten µL of the Sb_2Se_3 powder suspension (described above) was deposited on a target and then covered with paraffin solution in xylene (1 cm^2 of parafilm dissolved in 1 ml xylene).

Results and Discussion

LDI of different materials was used to generate clusters while mass spectra were recorded in both positive and negative ionisation modes by using a reflectron mass analyser. This analysis revealed that a low number of clusters and low-intensity spectra were produced in the negative ion mode. Therefore, the results obtained in the positive ion mode are presented.

Effect of laser energy on homemade Sb_2Se_3 polycrystalline material mass spectra

The effect of laser energy on intensity of clusters formed is shown in Figure 1. The high-intensity clusters were observed in the 300-450 *m/z* range; the intensities heightened as the laser energy increased. However, some low-intensity clusters were also observed in the 450-650 mass range (spectra not shown). This data indicates that the homemade Sb_2Se_3 polycrystalline material was rather easy to decompose even at relatively low laser energy (140 a.u.). Detailed analysis of the homemade Sb_2Se_3 polycrystalline material spectra is shown in Fig. S1A. In addition to $SbSe_2^+$, $Sb_2Se_n^+$ (n = 1, 2) and $Sb_3Se_n^+$ (n = 1-3) clusters, Sb_m^+ (m = 2-4) clusters were also detected. Comparison of experimental and theoretical isotopic patterns concerning Sb_3Se^+ are provided in Fig. S1B. Overall, they showed good agreement.

Effect of laser energy on thin film mass spectra

The effect of laser energy on thin film mass spectra (Fig. S2A) was different from that of homemade Sb_2Se_3 polycrystalline material. At 140 a.u. laser energy, the cluster intensities reached their maxima. The mass spectra showed that the thin film was less stable against pulsed laser irradiation than the homemade Sb_2Se_3 polycrystalline material. Further, the thin films were easier to ablate. An example of a thin film mass spectrum is shown in Figure 2. The thin film mass spectra showed similar clusters to those formed from the homemade Sb_2Se_3 polycrystalline material. However, the $Sb_3Se_3^+$, $SbSe_2^+$, Sb_m^+ (m = 2-4), $Sb_2Se_n^+$ (n = 1, 2) and $Sb_3Se_n^+$ (n = 1, 2) clusters were not observed. There was good agreement between the theoretical and experimental isotopic patterns concerning Sb_2Se^+cluster (Fig. S2B).

Effect of laser energy on commercial Sb_2Se_3 polycrystalline material mass spectra

Comparison of mass spectra generated from commercial Sb_2Se_3 polycrystalline bulk at different laser energies is shown in Figure 3. Even at low laser energy (120 a.u.), we observed several low-intensity clusters in the *m/z* range over 450. Fig. S3A shows the result of detailed mass spectra analysis concerning commercial Sb_2Se_3 polycrystalline bulk material. Besides $SbSe_2^+$, $Sb_2Se_n^+$ (n = 1-4) and $Sb_3Se_n^+$ (n = 1-5), Sb_m^+ (m = 3, 4) clusters were also noted. Comparison of experimental and theoretical isotopic patterns for the $Sb_2Se_2^+$ cluster is provided in Fig. S3B; there was good agreement between the experiment with the theoretical model.

Comparison of amorphous Sb_2Se_3 thin film, commercial and homemade polycrystalline Sb_2Se_3 material mass spectra

Figure 4 shows thin film, commercial and home-made polycrystalline Sb_2Se_3 material mass spectra that were measured using the same laser energy (120 a.u.). At this laser energy, the order of intensity was thin film, followed by homemade and finally commercial Sb_2Se_3 polycrystalline material, data that indicate the stability of the three materials with respect to the increasing laser pulse. In the homemade polycrystalline Sb_2Se_3 material and commercial Sb_2Se_3 polycrystalline bulk material mass spectra, the most intensive cluster was Sb_3Se^+. Comparatively, in the thin film mass spectra, the Sb_2Se^+ cluster was the strongest. The most intense cluster, observed in the thin film mass spectrum at 140–180 a.u. laser energy, was Sb_3Se^+. Additionally, the commercial Sb_2Se_3 polycrystalline bulk produced more clusters.

Special methods to enhance mass spectra intensity and produce higher-mass clusters

Enhancement of cluster intensity

GO, G or C_{60} were previously used as a matrix for SALDI mass spectrometry [25-27]. We examined whether these materials can increase the intensity of Sb_2Se_3 mass spectra. Comparison of mass spectra for commercial Sb_2Se_3 polycrystalline bulk and the same material deposited on the surface of GO, C_{60} or G at the same laser energy (120 a.u.) is shown in Figure 6. GO, G and C_{60} enhanced the intensity of the most of the signals present in mass spectra. GO was the most effective material for

enhancing the mass spectra intensity (9-times greater intensity compared to simple LDI), followed by C_{60} and then G.

Effect of paraffin

Comparison of commercial Sb_2Se_3 polycrystalline bulk mass spectra with and without a paraffin cover at 160 a.u. laser energy is shown in Figure 7A, B and C. At the *m/z* range below 510, the cluster intensities produced solely by Sb_2Se_3 was higher than when Sb_2Se_3 was covered with paraffin. On the contrary, in the *m/z* range over 510, the intensity of the clusters originating in Sb_2Se_3 covered with paraffin was higher than that one produced by Sb_2Se_3 alone. Furthermore, we detected the formation of new clusters beyond *m/z* 800 ($Sb_4Se_4^+$, $Sb_5Se_{3\text{-}6}^+$ and $Sb_7Se_4^+$) from Sb_2Se_3 covered with paraffin. Comparison of experimental and theoretical isotopic patterns for one newly identified $Sb_5Se_6^+$ cluster is given in Fig. S4; the data showed good agreement between the experimental results and theoretical model. The results obtained indicate that paraffin acts as a protective agent to diminish fragmentation. It is not easy to explain the effect of paraffines, as it can be very complex. First, because particles of materials are covered with paraffin layer which is absorbing part of the laser energy, the fragmentation is diminished. In addition, similarly to those of Ag^+ adducts with paraffines [28], we observed here the formation of $Sb_mSe_n^+$ cations adducts with paraffin ($C_4H_{10}{\cdot}Sb_2Se_3^+$ shown in Figure S5 A and $C_{18}H_{38}{\cdot}Sb_3Se^+$ shown in Figure S5 B). Such formation of charged adducts can also decrease the fragmentation. An overview of the Sb_m, Se_n and Sb_mSe_n clusters generated from all Sb_2Se_3 forms and Sb:Se mixtures (1:1 or 1:10) [23] is provided in Figure 5.

Conclusions

LDI with quadrupole ion trap time-of-flight mass spectrometry was used to characterise different Sb_2Se_3 forms (commercial or home-made polycrystalline material or amorphous thin films). We showed that this technique is a powerful method to study the formation of binary Sb_mSe_n clusters. Homemade Sb_2Se_3 polycrystalline material produced the lowest number of clusters during LDI. Commercial Sb_2Se_3 polycrystalline bulk generated a higher number of detected Sb_mSe_n species. The amorphous Sb_2Se_3 thin film was easily ablated. We demonstrated that GO, C60 or G are suitable materials for SALDI in order to enhance the mass spectra intensity of the clusters produced from Sb_2Se_3 polycrystalline material. With the use of paraffin, some new clusters were detected in the high-mass part of the spectra.

Acknowledgments

This work was funded with the support from the Czech Science Foundation (Projects No. 18-03823S).

References

[1] Tideswell, N.W., Kruse, F.H., McCullough, J.D.: The crystal structure of antimony selenide, Sb_2Se_3. Acta Cryst. **10**, 99-102 (1957)

[2] Voutsas, G.P., Papazoglou, A.G., Rentzeperis, P.J., Siapkas, D.: The crystal structure of antimony selenide, Sb_2Se_3. Z. Kristallogr. Cryst. Mater. **171**, 261-268 (1985)

[3] Vadapoo, R., Krishnan, S., Yilmaz, H., Marin, C.: Electronic structure of antimony selenide (Sb_2Se_3) from GW calculations. Phys. Status Solidi B. **3**, 700-705 (2011)

[4] Deringer, V.L., Stoffel, R.P., Wuttig, M., Dronskowski, R.: Vibrational properties and bonding nature of Sb_2Se_3 and their implications for chalcogenide materials. Chem. Sci. **6**, 5255-5262 (2015)

[5] Itoh, K.: Short- and medium-range order in Sb-Se glasses. J. Solid State Chem. **233**, 368-373 (2016)

[6] Holubová, H., Černošek, Z., Černosková, E.: The selenium based chalcogenide glasses with low content of As and Sb: DSC, StepScan DSC and Raman spectroscopy study. J. Non-Cryst. Solids. **355**, 2050-2053 (2009)

[7] Kostadinova, O., Yannopoulos, S.N.: Raman spectroscopic study of Sb_xSe_{100-x} phase-separated bulk glasses. J. Non-Cryst. Solids. **355**, 2040-2044 (2009)

[8] Halenkovič, T., Gutwirth, J., Němec, P., Baudet, E., Specht, M., Gueguen, Y., Sangleboeuf, J-C., Nazabal, V.: Amorphous Ge-Sb-Se thin films fabricated by co-sputtering: properties and photosensitivity. J. Am. Ceram. Soc. **101**, 2877-2887 (2018)

[9] Chen, C., Li, W.Q., Zhou, Y., Chen, C., Luo, M., Liu, X.S., Zeng, K., Yang, B., Zhang, C.W., H, J.B., Tang, J.: Optical properties of amorphous and polycrystalline Sb_2Se_3 thin films prepared by thermal evaporation. Appl Phys Lett. **107**, 043905 (2015)

[10] Němec, P., Olivier, M., Baudet, E., Kalendová, A., Benda, P., Nazabal, V.: Optical properties of $(GeSe_2)_{100-x}(Sb_2Se_3)_x$ glasses in near- and middle-infrared spectral regions. Mater. Res. Bull. **51**, 176-179 (2014)

[11] Baudet, E., Gutierrez-Arroyo, A., Němec, P., Bodiou, L., Lemaitre, J., De Sagazan, O., Lhermitte, H., Rinnert, E., Michel, K., Bureau, B., Charrier, J., Nazabal, V.: Selenide sputtered films development for MIR environmental sensor. Opt. Mater. Express. **6**, 2616-2627 (2016)

[12] Olivier, M., Němec, P., Boudebs, G., Boidin, R., Focsa, C., Nazabal. V.: Photosensitivity of pulsed laser deposited Ge-Sb-Se thin films. Opt. Mater. Express. **5**, 781-793 (2015)

[13] Baudet, E., Cardinaud, C., Boidin, R., Girard, A., Gutwirth, Jan., Němec, P., Nazabal, V.: X-ray photoelectron spectroscopy analysis of Ge–Sb–Se pulsed laser deposited thin films. J. Am. Ceram. Soc. **101**, 3347-3356 (2018)

[14] Malligavathy, M., Ananth Kumar, R.T., Das, Ch., Asokan, S., Pathinettam Padiyan, D.: Growth and characteristics of amorphous Sb_2Se_3 thin films of various thicknesses for memory switching applications. J. Non-Crystal. Solids. **429**, 93-97 (2015)

[15] Shylashree, N., Uma, B.V., Dhanush, S., Sagar, A., Nisarga, A., Aashith, K.,

Sangeetha, B.G.: Preparation and characterization of Sb_2Se_3 devices for memory applications. AIP Conference Proceedings. **1966**, 020032 (2018)

[16] Zhang, X., Korolkov, I., Fan, B., Cathelinaud, M., Ma, H., Adam, J.-L., Merdrignac, O., Calvez, L., Lhermite, H., Le Brizoual, L., Pasquinelli, M., Simon, J.-J.: Chalcogenide glass-ceramic with self-organized heterojunctions: application to photovoltaic solar cells. EPJ Photovoltaics. **9**, 3 (2018)

[17] Choi, Y., Mandal, T., Yang, W., Lee, Y., Im, S.H., Noh, J., Seok, S.: Sb_2Se_3-sensitized inorganic–organic heterojunction solar cells fabricated using a single-source precursor. Angew. Chem. **53**, 1329-1333 (2014)

[18] Zeng, K., Xue, D.-J., Tang, J.: Antimony selenide thin-film solar cells. Semicond. Sci. Tech. **31**, 063001 (2016)

[19] Hutter, O.S., Philips, L.J., Durose, K., Major, J.D.: 6.6% efficient antimony selenide solar cells using grain structure control and an organic contact layer. Sol. Energy Mater. Sol. Cells. **188**, 177-181 (2018)

[20] Carey, J.J., Allen, J. P., Scanlon, D.O., Watson, G.W.: The electronic structure of the antimony chalcogenide series: Prospects for optoelectronic applications. J. Solid State Chem. **213**, 116-125 (2014)

[21] Xue, M.-Zh., Fu, Zh.-W.: Pulsed laser deposited Sb_2Se_3 anode for lithium-ion batteries. J. Alloy Compd. **458**, 351–356 (2008)

[22] Ge, P., Cao, X., Hou, H., Li, S., Ji, X.: Rodlike Sb_2Se_3 wrapped with carbon: The exploring of electrochemical properties in sodium-ion batteries. ACS Appl. Mater. Interfaces. **9**, 34979-34989 (2017)

[23] Huang, F., Prokeš, L., Havel, J.: Laser ablation synthesis of antimony selenide clusters with simultaneous laser desorption ionization (LDI) quadrupole ion trap mass spectrometry. J. Am. Soc. Mass Spectrom. **30**, 634-638 (2019)

[24] Mawale, R.M., Ausekar, M.V., Prokeš, L., Nazabal, V., Baudet, E., Halenkovič, T., Bouška, M., Alberti, M., Němec, P., Havel, J.: Laser desorption ionization of As_2Ch_3 (Ch = S, Se, and Te) chalcogenides using quadrupole ion trap time-of-flight mass spectrometry: a comparative study. J. Am. Soc. Mass Spectrom. **28**, 2569-2579 (2017)

[25] Dong, X.L., Cheng, J.S., Li, J.H., Wang, Y.S.: Graphene as a novel matrix for the analysis of small molecules by MALDI-TOF MS. Anal. Chem. **82**, 6208-6214 (2010)

[26] Lee, G.b., Bae, S-E., Huh, S., and Cha, S.W.: Graphene oxide embedded sol–gel (GOSG) film as a SALDI MS substrate for robust metabolite fingerprinting. RSC Adv. **5**, 56455–56459 (2015)

[27] Liu, J.A., Xiong, L., Zhang, S., Wei, J.C., Xiong, S.X.: C_{60} fluorine derivative as novel matrix for small molecule analysis by MALDI-TOF MS. Metabolomics. **S1**, 002 (2012)

[28] Yang, M., Hashimoto, Kenro., Fujino, Tatsuya.: Silver nanoparticles loaded on ammonium exchanged zeolite as matrix for MALDI-TOF-MS analysis of short-chain n-alkanes. Chem. Phys. Lett. **706**, 525-532 (2018)

Figure captions

Figure 1. The effect of laser energy on the mass spectra from LDI of homemade Sb_2Se_3 polycrystalline material in the 300-500 *m/z* range in the positive ion mode.

Figure 2. Mass spectra from LDI of amorphous Sb_2Se_3 thin film in the 200-800 *m/z* range. The inset shows the magnification of spectra in 500-650 *m/z* range. Conditions: positive ion mode; 120 a.u. laser energy; * refers to unidentified clusters.

Figure 3. The effect of laser energy on the mass spectra from LDI of commercial Sb_2Se_3 polycrystalline bulk in the 300-500 *m/z* range in positive ion mode.

Figure 4. Mass spectra from LDI of commercial and homemade Sb_2Se_3 polycrystalline material as well as amorphous Sb_2Se_3 thin film in the 300-500*m/z* range. Conditions: positive ion mode; 120 a.u. laser energy.

Figure 5. Overview of clusters observed by using paraffin and Sb_mSe_n cluster stoichiometry generated from commercial/homemade Sb_2Se_3 polycrystalline material, amorphous Sb_2Se_3 thin film, and mixtures of antimony with selenium (Sb:Se = 1:1 or 1:10). ★New clusters by using paraffin; ○ Sb:Se = 1:10; ⬭ Sb:Se = 1:1; ▬ Thin film; ✦ Commercial polycrystalline Sb_2Se_3; ○ Home-made polycrystalline Sb_2Se_3.

Figure 6. Mass spectra from LDI of commercial polycrystalline Sb_2Se_3 on the surface of GO, C_{60}, G and on a common metal target in the 300-700 *m/z* range. Conditions: positive ion mode; 120 a.u. laser energy.

Figure 7A. Mass spectra from LDI of commercial polycrystalline Sb_2Se_3, and the same sample covered with paraffin, in the 310-510 *m/z* range. Conditions: positive ion

mode; 160 a.u. laser energy.

Figure 7B. Mass spectra from LDI of commercial polycrystalline Sb_2Se_3, and the same sample covered with paraffin, in the 510-790 *m/z* range. Conditions: positive ion mode; 160 a.u. laser energy.

Figure 7C. Mass spectra from LDI of commercial polycrystalline Sb_2Se_3, and the same sample covered with paraffin, in the 790-1300 *m/z* range. Conditions: positive ion mode; 160 a.u. laser energy.

Manuscript corrections in red

Click here to view linked References

Comparison of clusters produced from Sb_2Se_3 homemade polycrystalline material, thin films and commercial polycrystalline bulk using laser desorption ionisation with time of flight quadrupole ion trap mass spectrometry

Fei Huang,[1] Lubomír Prokeš,[1] Petr Němec,[2] Virginie Nazabal,[2,3] and Josef Havel[1*]

[1]Department of Chemistry, Faculty of Science, Masaryk University, Kamenice 5/A14, 62500 Brno, Czech Republic

[2]Department of Graphic Arts and Photophysics, Faculty of Chemical Technology, University of Pardubice, Studentská 573, 53210 Pardubice, Czech Republic

[3]Institut des Sciences Chimiques de Rennes, UMR-CNRS 6226, Equipe Verres et Céramiques, Université de Rennes 1, 35042 Rennes, France

*Author to whom correspondence should be addressed. Email: havel@chemi.muni.cz

Phone: +420 549494114, Fax: +420 549492494

Abstract. This study compared Sb_2Se_3 material in the form of commercial polycrystalline bulk, sputtered thin film and homemade polycrystalline material using laser desorption ionisation (LDI) time of flight mass spectrometry with quadrupole ion trap mass spectrometry. It also analysed the stoichiometry of the Sb_mSe_n clusters formed. The results showed that homemade Sb_2Se_3 bulk was more stable compared to thin film; its mass spectra showed the expected cluster formation. The use of materials for surface-assisted LDI (SALDI), i.e., graphene, graphene oxide and C_{60}, significantly increased the mass spectra intensity. In total, nineteen Sb_mSe_n clusters were observed. Six novel, high-mass clusters—$Sb_4Se_4^+$, $Sb_5Se_{3\text{-}6}^+$ and $Sb_7Se_4^+$—were observed for the first time when using paraffin as a protective agent.

Keywords: antimony selenide; clusters; laser desorption ionisation; paraffin; chalcogenides

Introduction

Sb_2Se_3, which is known in nature as the mineral antimonselite. The crystal and electronic structure of antimony selenide as well as its vibrational properties were previously determined [1-4]. Generally, the Sb_mSe_n system is an important member of chalcogenide materials. Under typical experimental conditions of chalcogenide glass synthesis, the glass-forming region in the Sb_mSe_n system is limited to rather low antimony content (up to 30%), and smaller glass batches often face phase separation problems [5-7]. On the other hand, it is possible to fabricate amorphous,

stoichiometric and thin Sb_2Se_3 films by physical vapour deposition techniques such as radio-frequency magnetron sputtering [8] or thermal evaporation [9]. Moreover, Sb_2Se_3 forms stable glasses and amorphous thin films with other glass-forming selenides like $GeSe_2$ [10-13]. Today, Sb_mSe_n materials, especially in the form of thin films, have been widely studied as amorphous thin films of Sb_2Se_3 for memory switching application [14-15], as glass-ceramic or antimony selenide thin films for solar cells [16-20], as Sb_2Se_3 anode for lithium, and sodium batteries [21-22].

In a previous article [23], we examined the formation of clusters produced by laser ablation from mixtures of Sb and Se elements in different ratios. We observed 24 Sb_mSe_n clusters that were generated from metal surface of common target. In this study, we would like to compare the stoichiometry of clusters formed by laser desorption ionisation (LDI) from Sb_2Se_3 materials in the form of commercial polycrystalline bulk, thin film, and homemade polycrystalline material to the clusters generated by laser ablation synthesis (LAS) from the mixtures of elements (antimony and selenium). Additionally, in order to evaluate the influence of various surfaces on cluster formation, some other materials that act as surface-assisted LDI (SALDI) matrices (graphene [G], graphene oxide [GO] and fullerene [C_{60}]) were used. Since paraffin (as a protective agent) was found to increase the intensity of chalcogenide high mass clusters [24], we also studied the assistance of paraffin in detail.

Experimental

Chemicals

Polycrystalline Sb_2Se_3 was purchased from Sigma-Aldrich (St. Louis, MO, USA). Homemade polycrystalline Sb_2Se_3 was synthesised using high-purity elements (Sb and Se of 99.999% purity). Acetonitrile, G, GO and C_{60} were purchased from Sigma-Aldrich (Steinheim, Germany). Parafilm was purchased from Bemis NA (Neenah, Wis., USA). Red phosphorus was obtained from Riedel de Haën (Hannover, Germany) and was purified via sublimation in a nitrogen atmosphere. Water was double distilled using a quartz apparatus from Heraeus Quarzschmelze (Hanau, Germany). All other reagents were of analytical-grade purity. Amorphous Sb_2Se_3 thin films were fabricated by radio-frequency magnetron sputtering using an MPE600S (Plassys-Bestek, France) multichamber physical vapour deposition system. For the depositions, single crystalline silicon <100> substrates and a polycrystalline Sb_2Se_3 sputtering target (99.999%, ALB Materials, USA) were employed. The experimental details of thin film deposition are provided elsewhere [8]. No Bragg peaks were detected in the X-ray diffraction patterns of deposited thin films, data that confirm their amorphous state.

Mass spectrometry

AXIMA Resonance and AXIMA CFR mass spectrometers, both from Kratos Analytical Ltd. (Manchester, UK), coupled with a quadrupole ion trap and time-of-flight detection, were used to record mass spectra in both positive and negative ion modes. Both instruments were equipped with a nitrogen laser (337 nm), and the laser repetition rate was set to 5 Hz with a pulse time width of 3 ns.

Software and computation

Launchpad software (Kompact version 2.9.3, 2011) from Kratos Analytical Ltd. (Manchester, UK) was used to determine Sb_mSe_n cluster stoichiometry via comparison of isotopic envelopes.

Sample preparation for mass spectrometry

1. Commercial Sb_2Se_3 polycrystalline bulk, homemade polycrystalline material and amorphous Sb_2Se_3 thin film

An agate mortar was used to pulverise the polycrystalline Sb_2Se_3; the powder was then suspended in acetonitrile (1 mg/ml). From the prepared suspensions, 10 µL was deposited on a MALDI target and dried in open air. The amorphous Sb_2Se_3 thin film was fixed on the target with a narrow piece of parafilm.

2. SALDI using GO, G and C_{60} surfaces

Ten µL of GO, G, or C_{60} suspensions in acetonitrile were separately deposited on individual spots of a MALDI target, and then 10 µL of the commercial polycrystalline bulk Sb_2Se_3 powder suspension (described above) was separately added on the surface of the GO, G or C_{60} suspension.

3. Sb_2Se_3 covered with paraffin

Ten µL of the Sb_2Se_3 powder suspension (described above) was deposited on a target and then covered with paraffin solution in xylene (1 cm^2 of parafilm dissolved in 1 ml xylene).

Results and Discussion

LDI of different materials was used to generate clusters while mass spectra were recorded in both positive and negative ionisation modes by using a reflectron mass analyser. This analysis revealed that a low number of clusters and low-intensity spectra were produced in the negative ion mode. Therefore, the results obtained in the positive ion mode are presented.

Effect of laser energy on homemade Sb_2Se_3 polycrystalline material mass spectra

The effect of laser energy on intensity of clusters formed is shown in Figure 1. The high-intensity clusters were observed in the 300-450 *m/z* range; the intensities heightened as the laser energy increased. However, some low-intensity clusters were also observed in the 450-650 mass range (spectra not shown). This data indicates that the homemade Sb_2Se_3 polycrystalline material was rather easy to decompose even at relatively low laser energy (140 a.u.). Detailed analysis of the homemade Sb_2Se_3 polycrystalline material spectra is shown in Fig. S1A. In addition to $SbSe_2^+$, $Sb_2Se_n^+$ (n = 1, 2) and $Sb_3Se_n^+$ (n = 1-3) clusters, Sb_m^+ (m = 2-4) clusters were also detected. Comparison of experimental and theoretical isotopic patterns concerning Sb_3Se^+ are provided in Fig. S1B. Overall, they showed good agreement.

Effect of laser energy on thin film mass spectra

The effect of laser energy on thin film mass spectra (Fig. S2A) was different from that of homemade Sb_2Se_3 polycrystalline material. At 140 a.u. laser energy, the cluster intensities reached their maxima. The mass spectra showed that the thin film was less stable against pulsed laser irradiation than the homemade Sb_2Se_3 polycrystalline material. Further, the thin films were easier to ablate. An example of a thin film mass spectrum is shown in Figure 2. The thin film mass spectra showed similar clusters to those formed from the homemade Sb_2Se_3 polycrystalline material. However, the $Sb_3Se_3^+$, $SbSe_2^+$, Sb_m^+ (m = 2-4), $Sb_2Se_n^+$ (n = 1, 2) and $Sb_3Se_n^+$ (n = 1, 2) clusters were not observed. There was good agreement between the theoretical and experimental isotopic patterns concerning Sb_2Se^+cluster (Fig. S2B).

Effect of laser energy on commercial Sb_2Se_3 polycrystalline material mass spectra

Comparison of mass spectra generated from commercial Sb_2Se_3 polycrystalline bulk at different laser energies is shown in Figure 3. Even at low laser energy (120 a.u.), we observed several low-intensity clusters in the *m/z* range over 450. Fig. S3A shows the result of detailed mass spectra analysis concerning commercial Sb_2Se_3 polycrystalline bulk material. Besides $SbSe_2^+$, $Sb_2Se_n^+$ (n = 1-4) and $Sb_3Se_n^+$ (n = 1-5), Sb_m^+ (m = 3, 4) clusters were also noted. Comparison of experimental and theoretical isotopic patterns for the $Sb_2Se_2^+$ cluster is provided in Fig. S3B; there was good agreement between the experiment with the theoretical model.

Comparison of amorphous Sb_2Se_3 thin film, commercial and homemade polycrystalline Sb_2Se_3 material mass spectra

Figure 4 shows thin film, commercial and home-made polycrystalline Sb_2Se_3 material mass spectra that were measured using the same laser energy (120 a.u.). At this laser energy, the order of intensity was thin film, followed by homemade and finally commercial Sb_2Se_3 polycrystalline material, data that indicate the stability of the three materials with respect to the increasing laser pulse. In the homemade polycrystalline Sb_2Se_3 material and commercial Sb_2Se_3 polycrystalline bulk material mass spectra, the most intensive cluster was Sb_3Se^+. Comparatively, in the thin film mass spectra, the Sb_2Se^+ cluster was the strongest. The most intense cluster, observed in the thin film mass spectrum at 140–180 a.u. laser energy, was Sb_3Se^+. Additionally, the commercial Sb_2Se_3 polycrystalline bulk produced more clusters.

Special methods to enhance mass spectra intensity and produce higher-mass clusters

Enhancement of cluster intensity

GO, G or C_{60} were previously used as a matrix for SALDI mass spectrometry [25-27]. We examined whether these materials can increase the intensity of Sb_2Se_3 mass spectra. Comparison of mass spectra for commercial Sb_2Se_3 polycrystalline bulk and the same material deposited on the surface of GO, C_{60} or G at the same laser energy (120 a.u.) is shown in Figure 6. GO, G and C_{60} enhanced the intensity of the most of the signals present in mass spectra. GO was the most effective material for

enhancing the mass spectra intensity (9-times greater intensity compared to simple LDI), followed by C_{60} and then G.

Effect of paraffin

Comparison of commercial Sb_2Se_3 polycrystalline bulk mass spectra with and without a paraffin cover at 160 a.u. laser energy is shown in Figure 7A, B and C. At the *m/z* range below 510, the cluster intensities produced solely by Sb_2Se_3 was higher than when Sb_2Se_3 was covered with paraffin. On the contrary, in the *m/z* range over 510, the intensity of the clusters originating in Sb_2Se_3 covered with paraffin was higher than that one produced by Sb_2Se_3 alone. Furthermore, we detected the formation of new clusters beyond *m/z* 800 ($Sb_4Se_4^+$, $Sb_5Se_{3\text{-}6}^+$ and $Sb_7Se_4^+$) from Sb_2Se_3 covered with paraffin. Comparison of experimental and theoretical isotopic patterns for one newly identified $Sb_5Se_6^+$ cluster is given in Fig. S4; the data showed good agreement between the experimental results and theoretical model. The results obtained indicate that paraffin acts as a protective agent to diminish fragmentation. It is not easy to explain the effect of paraffines, as it can be very complex. First, because particles of materials are covered with paraffin layer which is absorbing part of the laser energy, the fragmentation is diminished. In addition, similarly to those of Ag^+ adducts with paraffines [28], we observed here the formation of $Sb_mSe_n^+$ cations adducts with paraffin ($C_4H_{10}{\cdot}Sb_2Se_3^+$ shown in Figure S5 A and $C_{18}H_{38}{\cdot}Sb_3Se^+$ shown in Figure S5 B). Such formation of charged adducts can also decrease the fragmentation. An overview of the Sb_m, Se_n and Sb_mSe_n clusters generated from all Sb_2Se_3 forms and Sb:Se mixtures (1:1 or 1:10) [23] is provided in Figure 5.

Conclusions

LDI with quadrupole ion trap time-of-flight mass spectrometry was used to characterise different Sb_2Se_3 forms (commercial or home-made polycrystalline material or amorphous thin films). We showed that this technique is a powerful method to study the formation of binary Sb_mSe_n clusters. Homemade Sb_2Se_3 polycrystalline material produced the lowest number of clusters during LDI. Commercial Sb_2Se_3 polycrystalline bulk generated a higher number of detected Sb_mSe_n species. The amorphous Sb_2Se_3 thin film was easily ablated. We demonstrated that GO, C60 or G are suitable materials for SALDI in order to enhance the mass spectra intensity of the clusters produced from Sb_2Se_3 polycrystalline material. With the use of paraffin, some new clusters were detected in the high-mass part of the spectra.

Acknowledgments

This work was funded with the support from the Czech Science Foundation (Projects No. 18-03823S).

References

[1] Tideswell, N.W., Kruse, F.H., McCullough, J.D.: The crystal structure of antimony selenide, Sb_2Se_3. Acta Cryst. **10**, 99-102 (1957)

[2] Voutsas, G.P., Papazoglou, A.G., Rentzeperis, P.J., Siapkas, D.: The crystal structure of antimony selenide, Sb_2Se_3. Z. Kristallogr. Cryst. Mater. **171**, 261-268 (1985)

[3] Vadapoo, R., Krishnan, S., Yilmaz, H., Marin, C.: Electronic structure of antimony selenide (Sb_2Se_3) from GW calculations. Phys. Status Solidi B. **3**, 700-705 (2011)

[4] Deringer, V.L., Stoffel, R.P., Wuttig, M., Dronskowski, R.: Vibrational properties and bonding nature of Sb_2Se_3 and their implications for chalcogenide materials. Chem. Sci. **6**, 5255-5262 (2015)

[5] Itoh, K.: Short- and medium-range order in Sb-Se glasses. J. Solid State Chem. **233**, 368-373 (2016)

[6] Holubová, H., Černošek, Z., Černosková, E.: The selenium based chalcogenide glasses with low content of As and Sb: DSC, StepScan DSC and Raman spectroscopy study. J. Non-Cryst. Solids. **355**, 2050-2053 (2009)

[7] Kostadinova, O., Yannopoulos, S.N.: Raman spectroscopic study of Sb_xSe_{100-x} phase-separated bulk glasses. J. Non-Cryst. Solids. **355**, 2040-2044 (2009)

[8] Halenkovič, T., Gutwirth, J., Němec, P., Baudet, E., Specht, M., Gueguen, Y., Sangleboeuf, J-C., Nazabal, V.: Amorphous Ge-Sb-Se thin films fabricated by co-sputtering: properties and photosensitivity. J. Am. Ceram. Soc. **101**, 2877-2887 (2018)

[9] Chen, C., Li, W.Q., Zhou, Y., Chen, C., Luo, M., Liu, X.S., Zeng, K., Yang, B., Zhang, C.W., H, J.B., Tang, J.: Optical properties of amorphous and polycrystalline Sb_2Se_3 thin films prepared by thermal evaporation. Appl Phys Lett. **107**, 043905 (2015)

[10] Němec, P., Olivier, M., Baudet, E., Kalendová, A., Benda, P., Nazabal, V.: Optical properties of $(GeSe_2)_{100-x}(Sb_2Se_3)_x$ glasses in near- and middle-infrared spectral regions. Mater. Res. Bull. **51**, 176-179 (2014)

[11] Baudet, E., Gutierrez-Arroyo, A., Němec, P., Bodiou, L., Lemaitre, J., De Sagazan, O., Lhermitte, H., Rinnert, E., Michel, K., Bureau, B., Charrier, J., Nazabal, V.: Selenide sputtered films development for MIR environmental sensor. Opt. Mater. Express. **6**, 2616-2627 (2016)

[12] Olivier, M., Němec, P., Boudebs, G., Boidin, R., Focsa, C., Nazabal. V.: Photosensitivity of pulsed laser deposited Ge-Sb-Se thin films. Opt. Mater. Express. **5**, 781-793 (2015)

[13] Baudet, E., Cardinaud, C., Boidin, R., Girard, A., Gutwirth, Jan., Němec, P., Nazabal, V.: X-ray photoelectron spectroscopy analysis of Ge–Sb–Se pulsed laser deposited thin films. J. Am. Ceram. Soc. **101**, 3347-3356 (2018)

[14] Malligavathy, M., Ananth Kumar, R.T., Das, Ch., Asokan, S., Pathinettam Padiyan, D.: Growth and characteristics of amorphous Sb_2Se_3 thin films of various thicknesses for memory switching applications. J. Non-Crystal. Solids. **429**, 93-97 (2015)

[15] Shylashree, N., Uma, B.V., Dhanush, S., Sagar, A., Nisarga, A., Aashith, K.,

Sangeetha, B.G.: Preparation and characterization of Sb_2Se_3 devices for memory applications. AIP Conference Proceedings. **1966**, 020032 (2018)

[16] Zhang, X., Korolkov, I., Fan, B., Cathelinaud, M., Ma, H., Adam, J.-L., Merdrignac, O., Calvez, L., Lhermite, H., Le Brizoual, L., Pasquinelli, M., Simon, J.-J.: Chalcogenide glass-ceramic with self-organized heterojunctions: application to photovoltaic solar cells. EPJ Photovoltaics. **9**, 3 (2018)

[17] Choi, Y., Mandal, T., Yang, W., Lee, Y., Im, S.H., Noh, J., Seok, S.: Sb_2Se_3-sensitized inorganic–organic heterojunction solar cells fabricated using a single-source precursor. Angew. Chem. **53**, 1329-1333 (2014)

[18] Zeng, K., Xue, D.-J., Tang, J.: Antimony selenide thin-film solar cells. Semicond. Sci. Tech. **31**, 063001 (2016)

[19] Hutter, O.S., Philips, L.J., Durose, K., Major, J.D.: 6.6% efficient antimony selenide solar cells using grain structure control and an organic contact layer. Sol. Energy Mater. Sol. Cells. **188**, 177-181 (2018)

[20] Carey, J.J., Allen, J. P., Scanlon, D.O., Watson, G.W.: The electronic structure of the antimony chalcogenide series: Prospects for optoelectronic applications. J. Solid State Chem. **213**, 116-125 (2014)

[21] Xue, M.-Zh., Fu, Zh.-W.: Pulsed laser deposited Sb_2Se_3 anode for lithium-ion batteries. J. Alloy Compd. **458**, 351–356 (2008)

[22] Ge, P., Cao, X., Hou, H., Li, S., Ji, X.: Rodlike Sb_2Se_3 wrapped with carbon: The exploring of electrochemical properties in sodium-ion batteries. ACS Appl. Mater. Interfaces. **9**, 34979-34989 (2017)

[23] Huang, F., Prokeš, L., Havel, J.: Laser ablation synthesis of antimony selenide clusters with simultaneous laser desorption ionization (LDI) quadrupole ion trap mass spectrometry. J. Am. Soc. Mass Spectrom. **30**, 634-638 (2019)

[24] Mawale, R.M., Ausekar, M.V., Prokeš, L., Nazabal, V., Baudet, E., Halenkovič, T., Bouška, M., Alberti, M., Němec, P., Havel, J.: Laser desorption ionization of As_2Ch_3 (Ch = S, Se, and Te) chalcogenides using quadrupole ion trap time-of-flight mass spectrometry: a comparative study. J. Am. Soc. Mass Spectrom. **28**, 2569-2579 (2017)

[25] Dong, X.L., Cheng, J.S., Li, J.H., Wang, Y.S.: Graphene as a novel matrix for the analysis of small molecules by MALDI-TOF MS. Anal. Chem. **82**, 6208-6214 (2010)

[26] Lee, G.b., Bae, S-E., Huh, S., and Cha, S.W.: Graphene oxide embedded sol–gel (GOSG) film as a SALDI MS substrate for robust metabolite fingerprinting. RSC Adv. **5**, 56455–56459 (2015)

[27] Liu, J.A., Xiong, L., Zhang, S., Wei, J.C., Xiong, S.X.: C_{60} fluorine derivative as novel matrix for small molecule analysis by MALDI-TOF MS. Metabolomics. **S1**, 002 (2012)

[28] Yang, M., Hashimoto, Kenro., Fujino, Tatsuya.: Silver nanoparticles loaded on ammonium exchanged zeolite as matrix for MALDI-TOF-MS analysis of short-chain n-alkanes. Chem. Phys. Lett. **706**, 525-532 (2018)

Figure captions

Figure 1. The effect of laser energy on the mass spectra from LDI of homemade Sb_2Se_3 polycrystalline material in the 300-500 *m/z* range in the positive ion mode.

Figure 2. Mass spectra from LDI of amorphous Sb_2Se_3 thin film in the 200-800 *m/z* range. The inset shows the magnification of spectra in 500-650 *m/z* range. Conditions: positive ion mode; 120 a.u. laser energy; * refers to unidentified clusters.

Figure 3. The effect of laser energy on the mass spectra from LDI of commercial Sb_2Se_3 polycrystalline bulk in the 300-500 *m/z* range in positive ion mode.

Figure 4. Mass spectra from LDI of commercial and homemade Sb_2Se_3 polycrystalline material as well as amorphous Sb_2Se_3 thin film in the 300-500*m/z* range. Conditions: positive ion mode; 120 a.u. laser energy.

Figure 5. Overview of clusters observed by using paraffin and Sb_mSe_n cluster stoichiometry generated from commercial/homemade Sb_2Se_3 polycrystalline material, amorphous Sb_2Se_3 thin film, and mixtures of antimony with selenium (Sb:Se = 1:1 or 1:10). ★New clusters by using paraffin; ○ Sb:Se = 1:10; ⬭ Sb:Se = 1:1; ▬ Thin film; ✦ Commercial polycrystalline Sb_2Se_3; ◯ Home-made polycrystalline Sb_2Se_3.

Figure 6. Mass spectra from LDI of commercial polycrystalline Sb_2Se_3 on the surface of GO, C_{60}, G and on a common metal target in the 300-700 *m/z* range. Conditions: positive ion mode; 120 a.u. laser energy.

Figure 7A. Mass spectra from LDI of commercial polycrystalline Sb_2Se_3, and the same sample covered with paraffin, in the 310-510 *m/z* range. Conditions: positive ion

mode; 160 a.u. laser energy.

Figure 7B. Mass spectra from LDI of commercial polycrystalline Sb_2Se_3, and the same sample covered with paraffin, in the 510-790 *m/z* range. Conditions: positive ion mode; 160 a.u. laser energy.

Figure 7C. Mass spectra from LDI of commercial polycrystalline Sb_2Se_3, and the same sample covered with paraffin, in the 790-1300 *m/z* range. Conditions: positive ion mode; 160 a.u. laser energy.

Figure 1

Click here to access/download;Figures;Figure 1.jpg

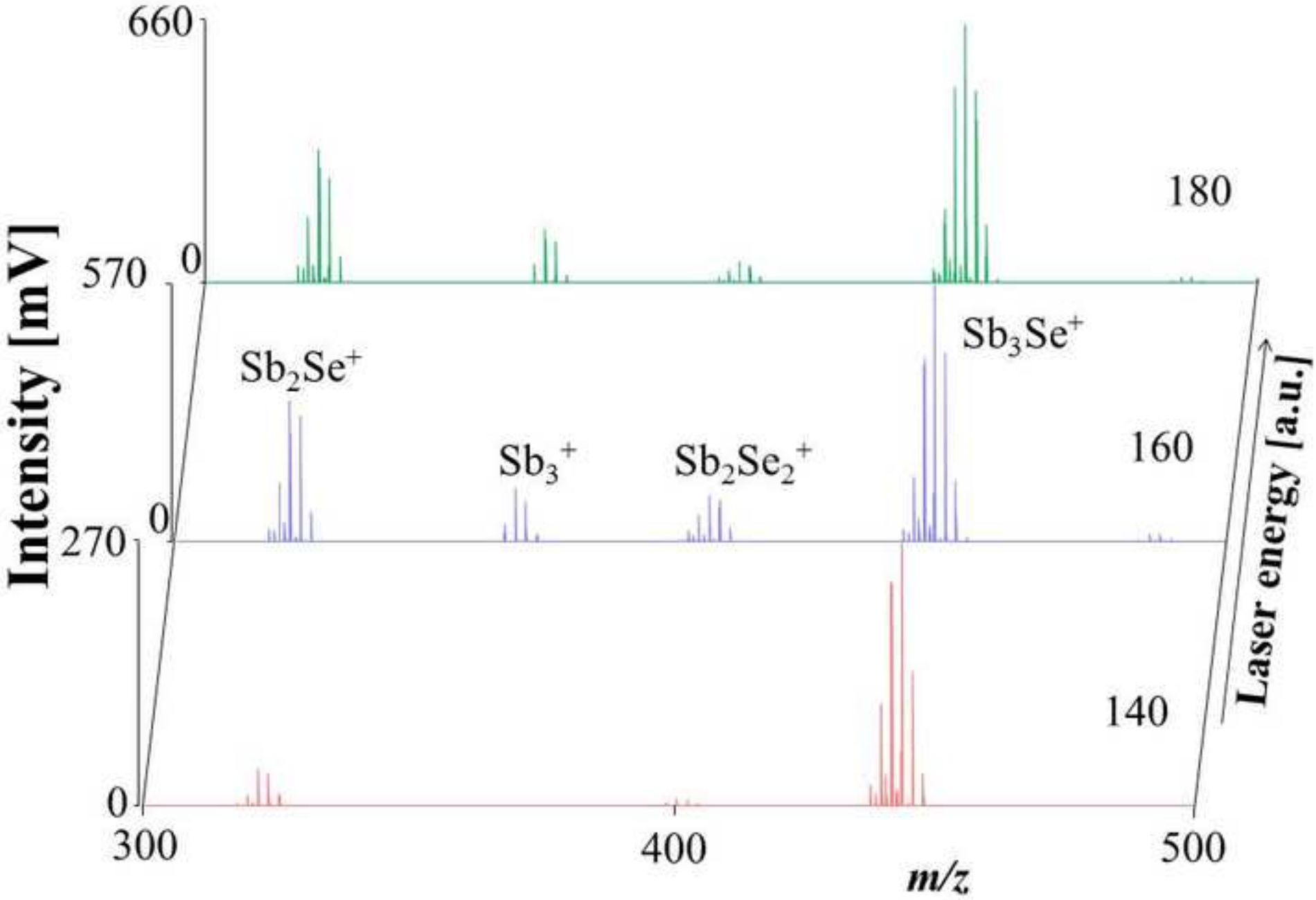

Figure 2

Click here to access/download;Figures;Figure 2.jpg

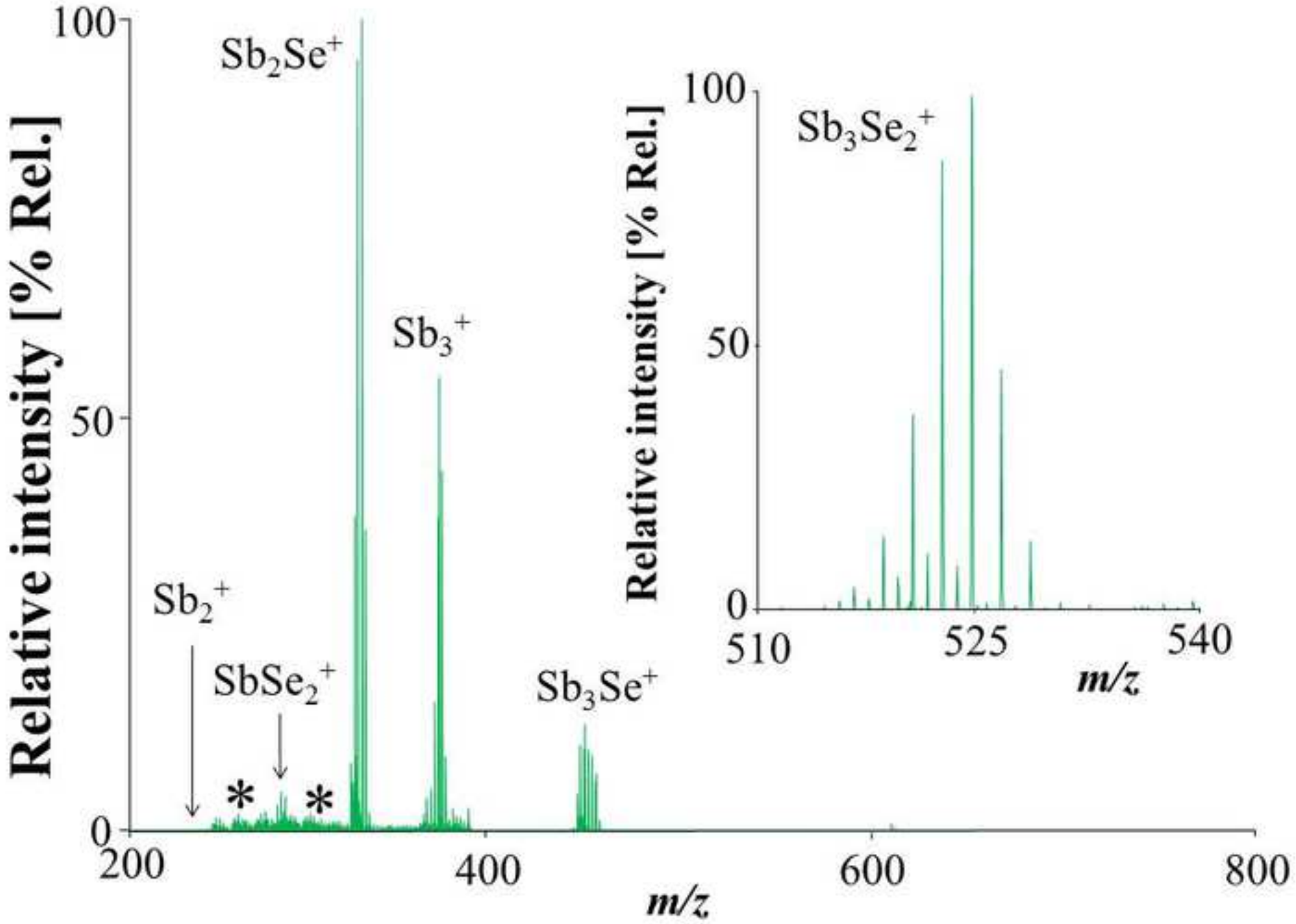

Figure 3

Click here to access/download;Figures;Figure 3.jpg

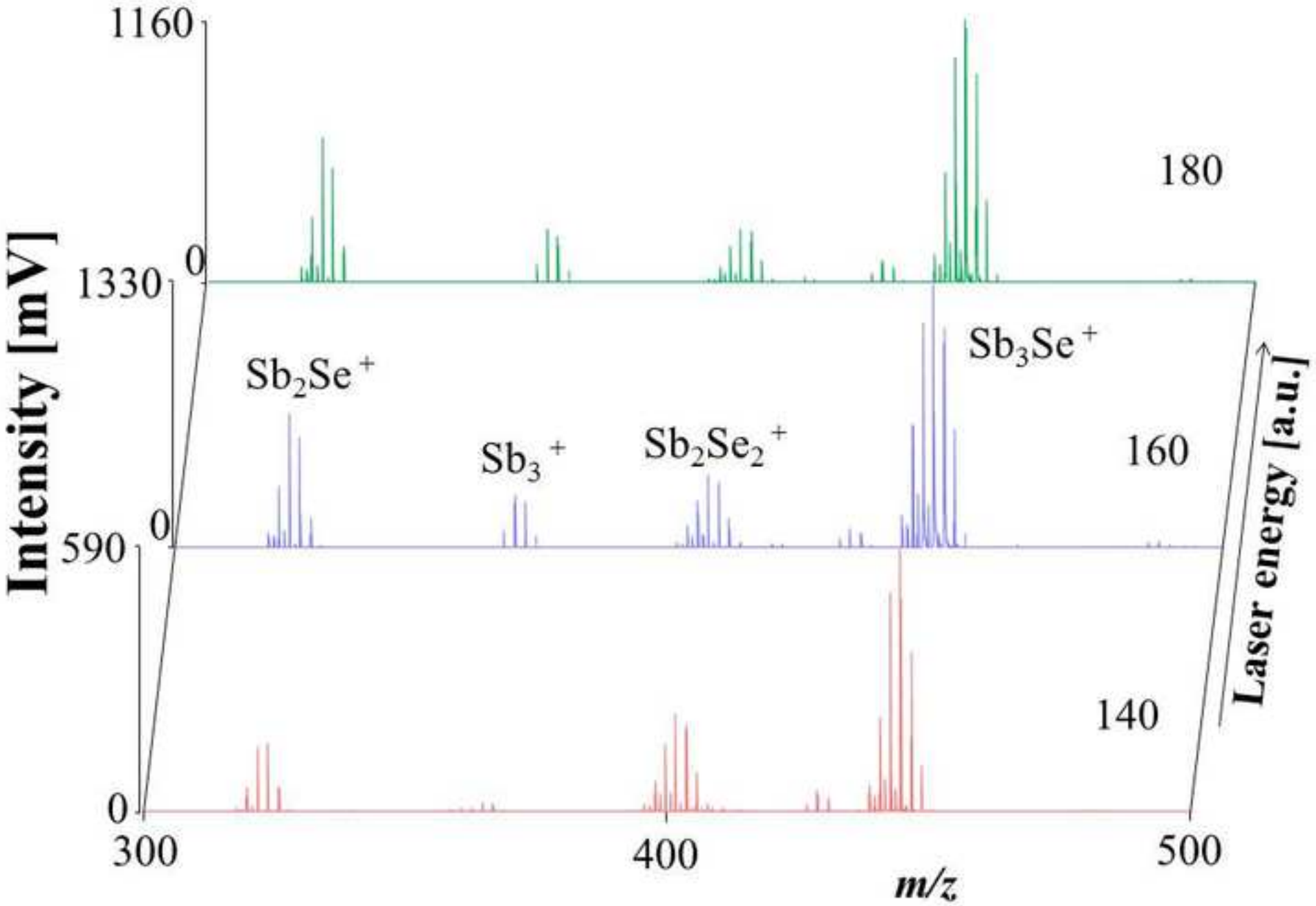

Figure 4

Click here to access/download;Figures;Figure 4.jpg

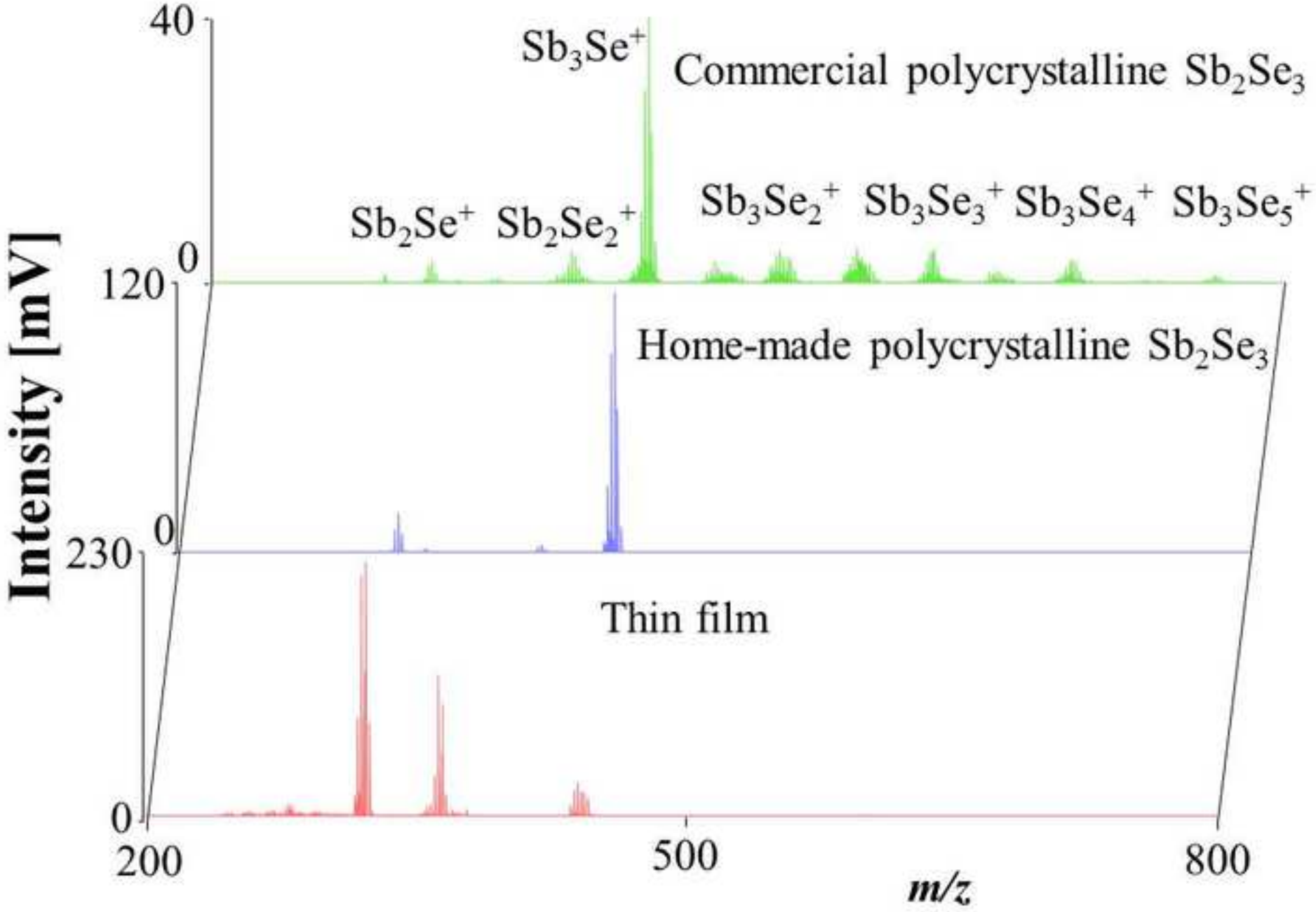

Figure 5

Click here to access/download;Figures;Figure 5.jpg

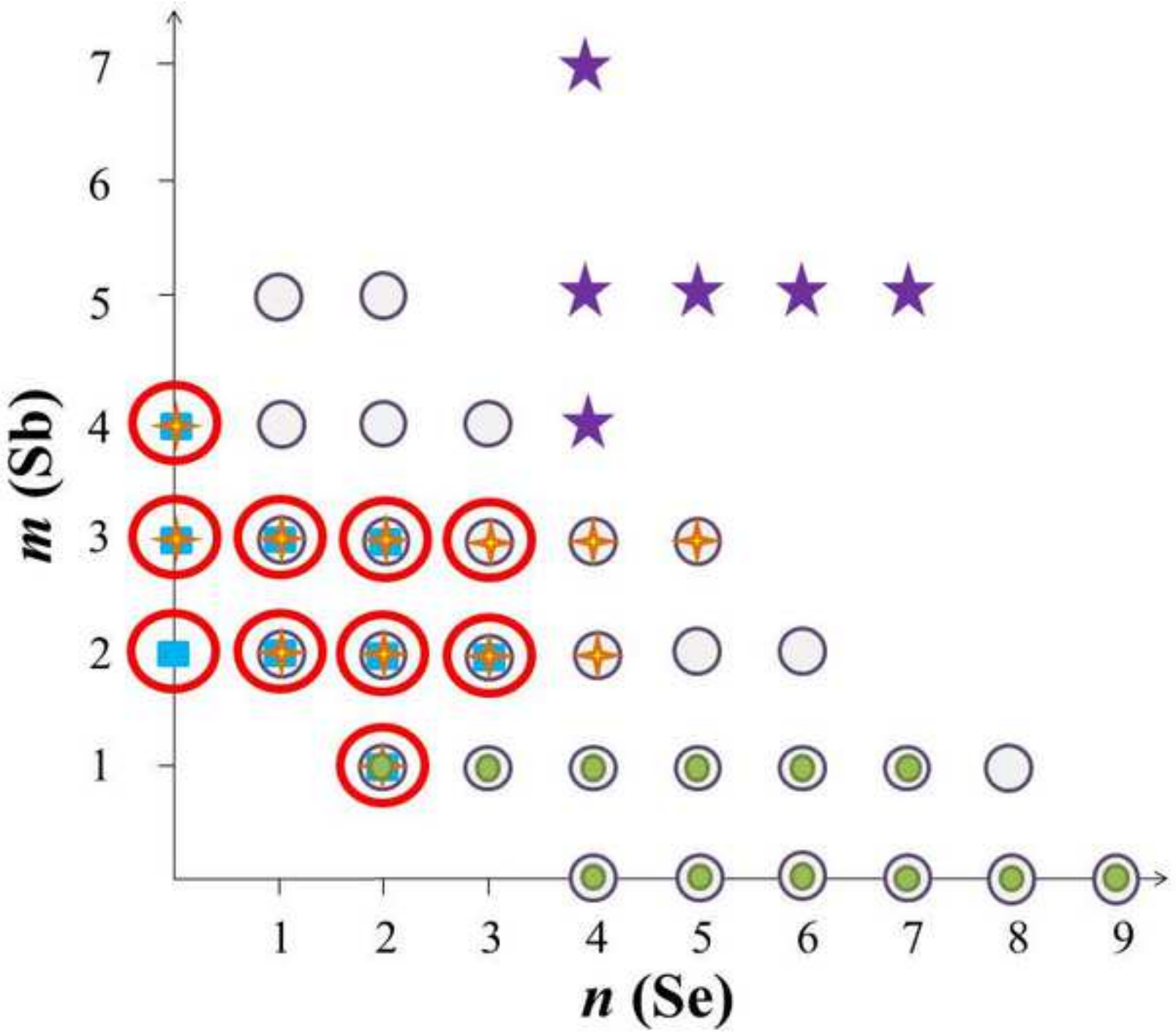

Figure 6

Click here to access/download;Figures;Figure 6.jpg

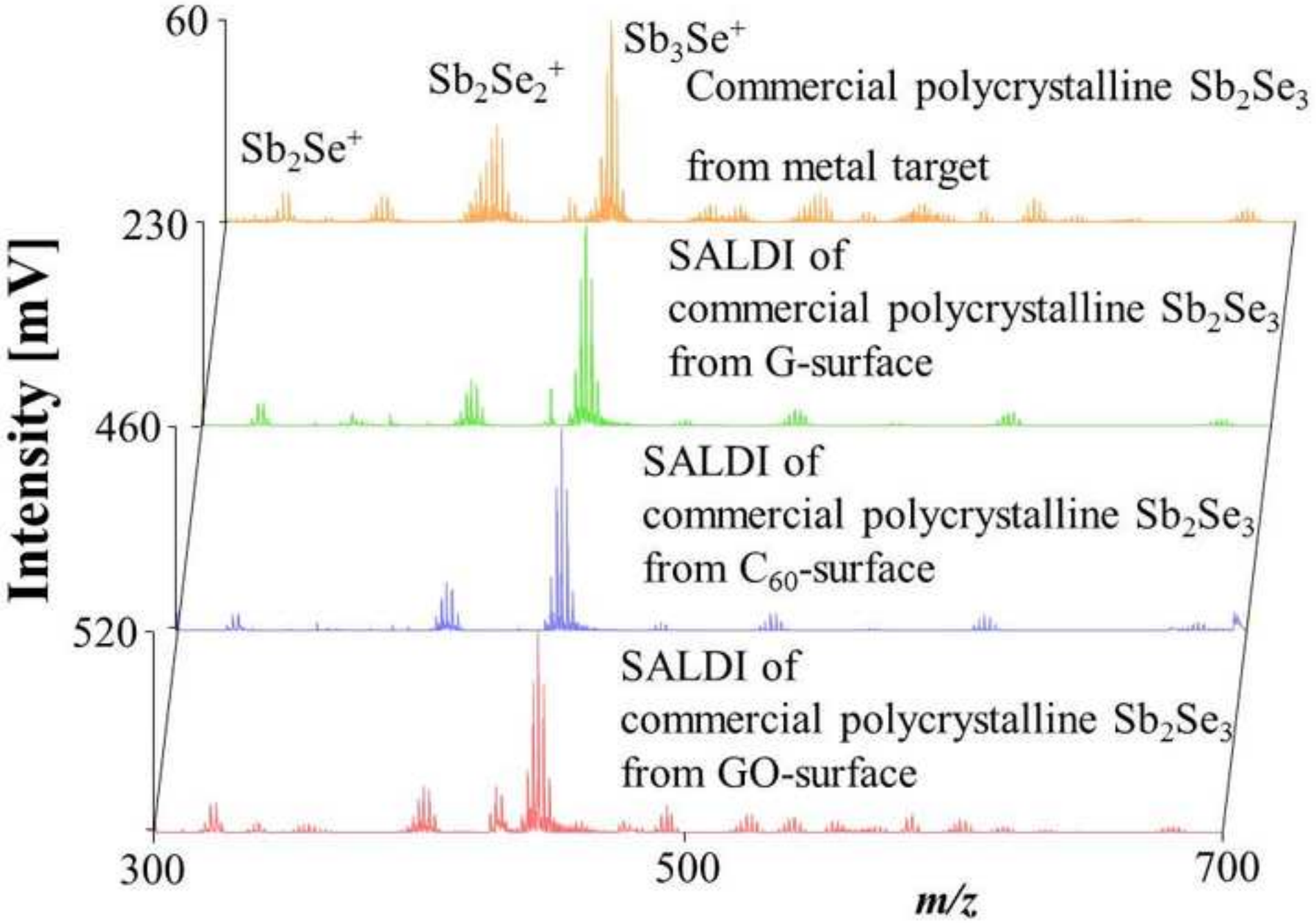

Figure 7A

Click here to access/download;Figures;Figure 7A.jpg

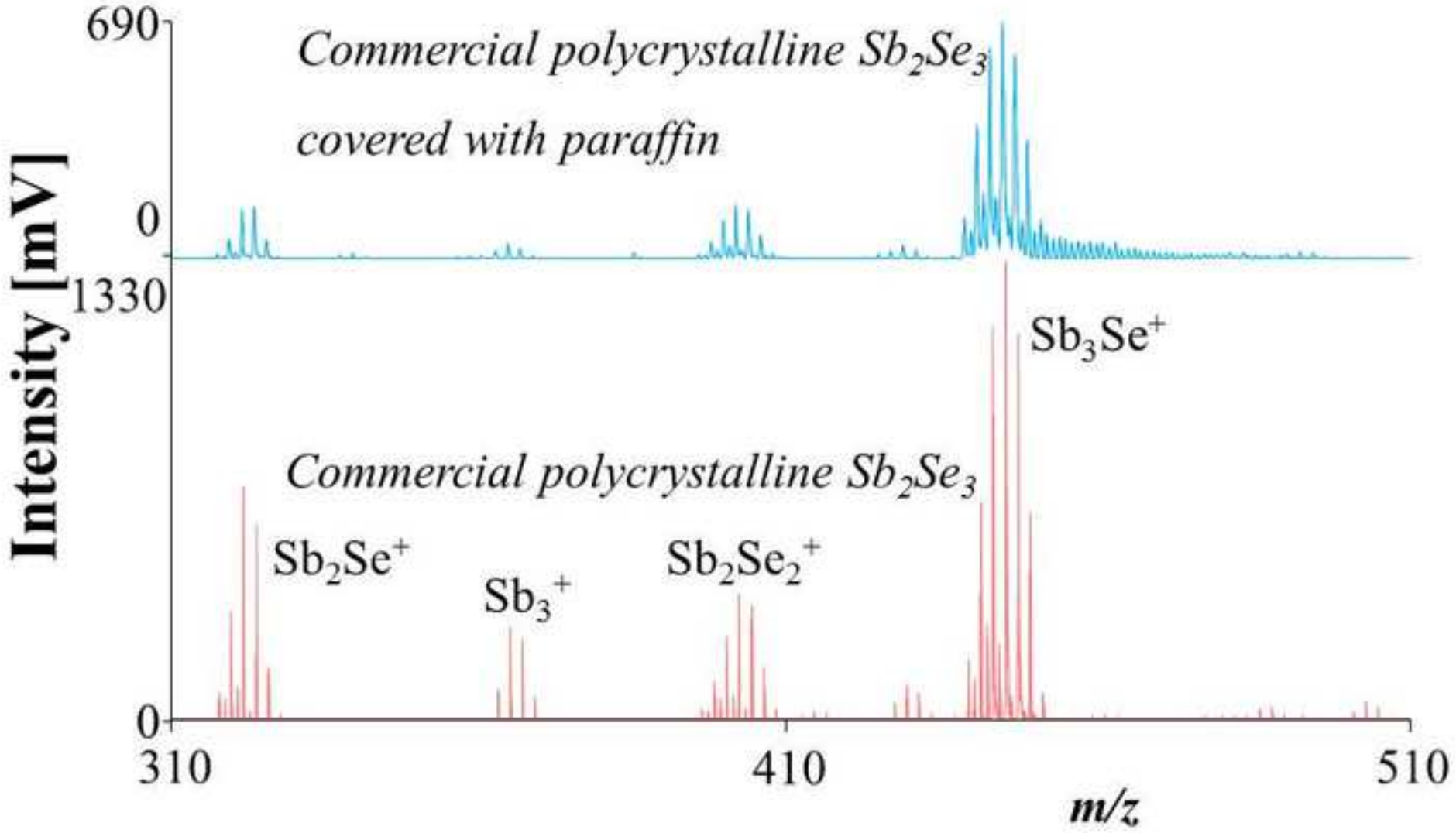

Figure 7B

Click here to access/download;Figures;Figure 7B.jpg

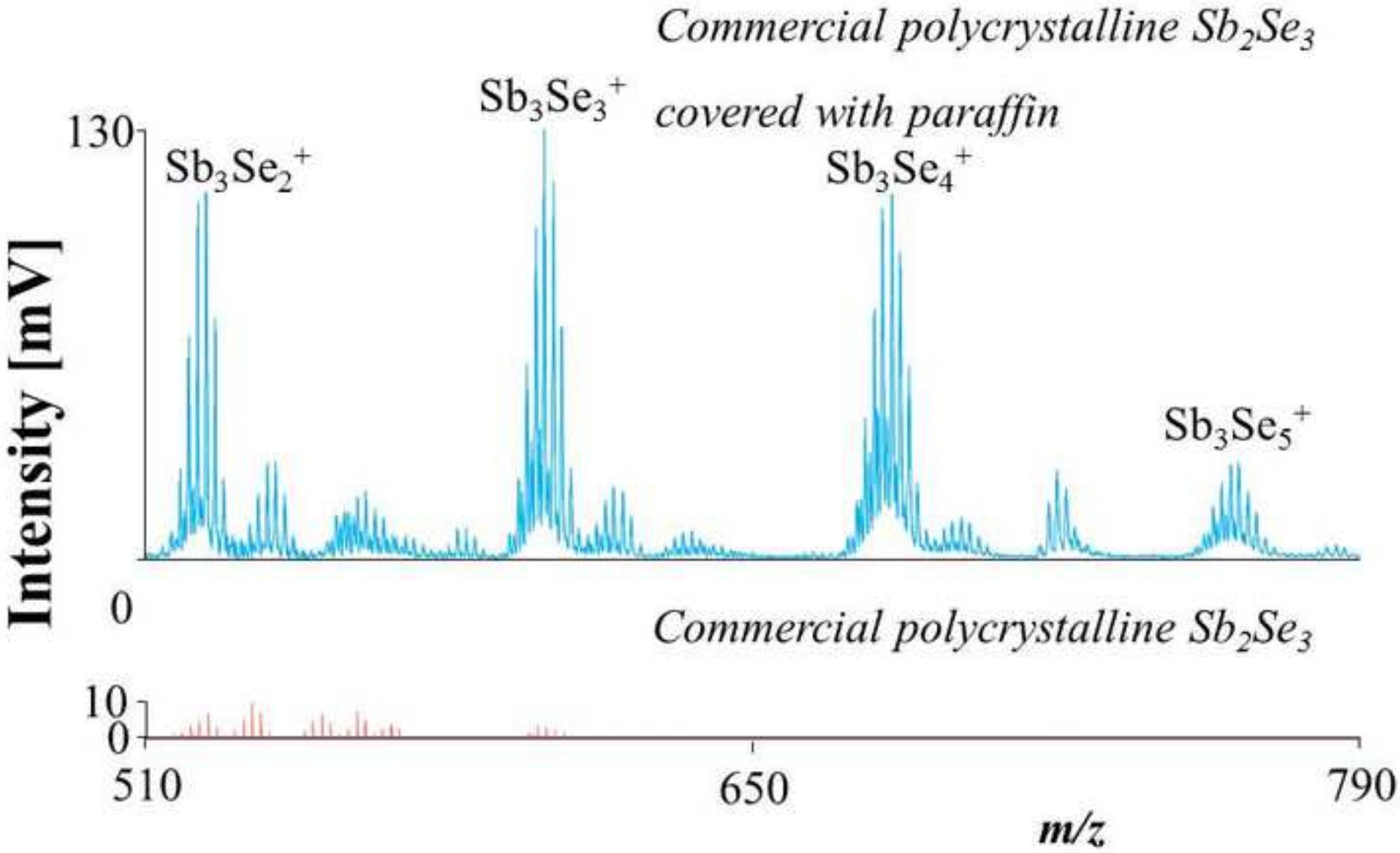

Figure 7C

Click here to access/download;Figures;Figure 7C.jpg

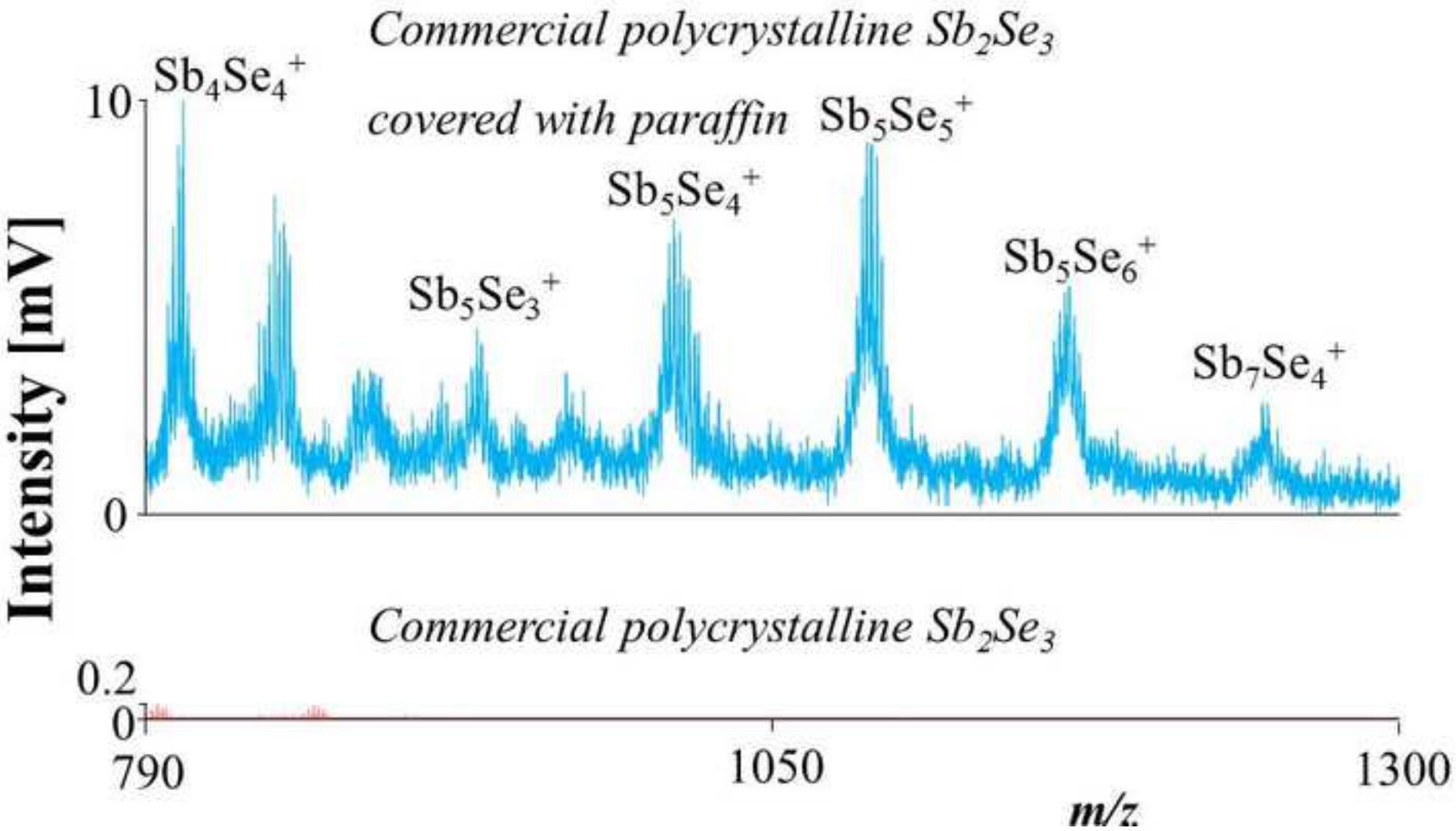

Figure S1A

Click here to access/download;Figures;Figure S1 A.jpg

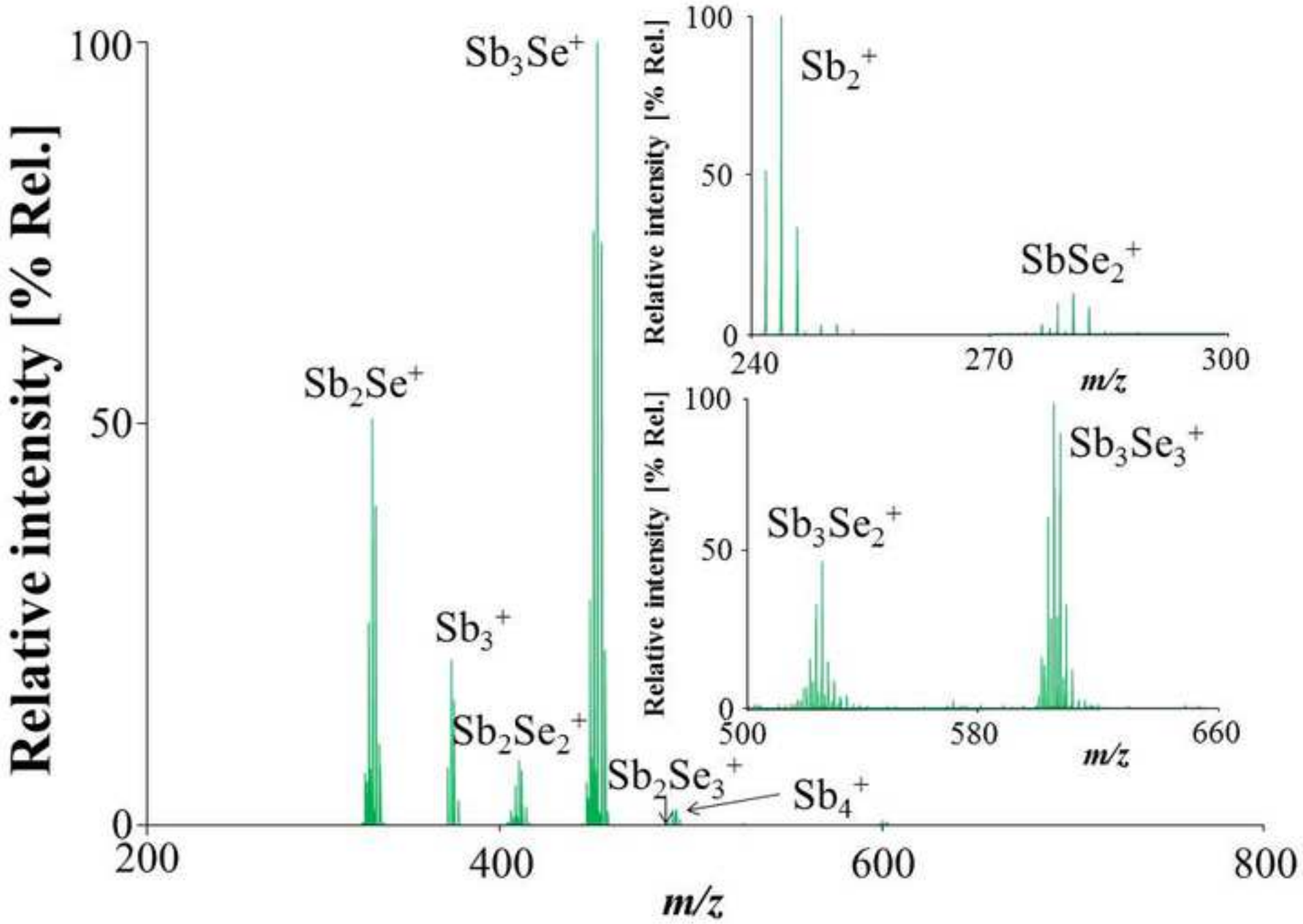

Figure S1B

Click here to access/download;Figures;Figure S1 B.jpg

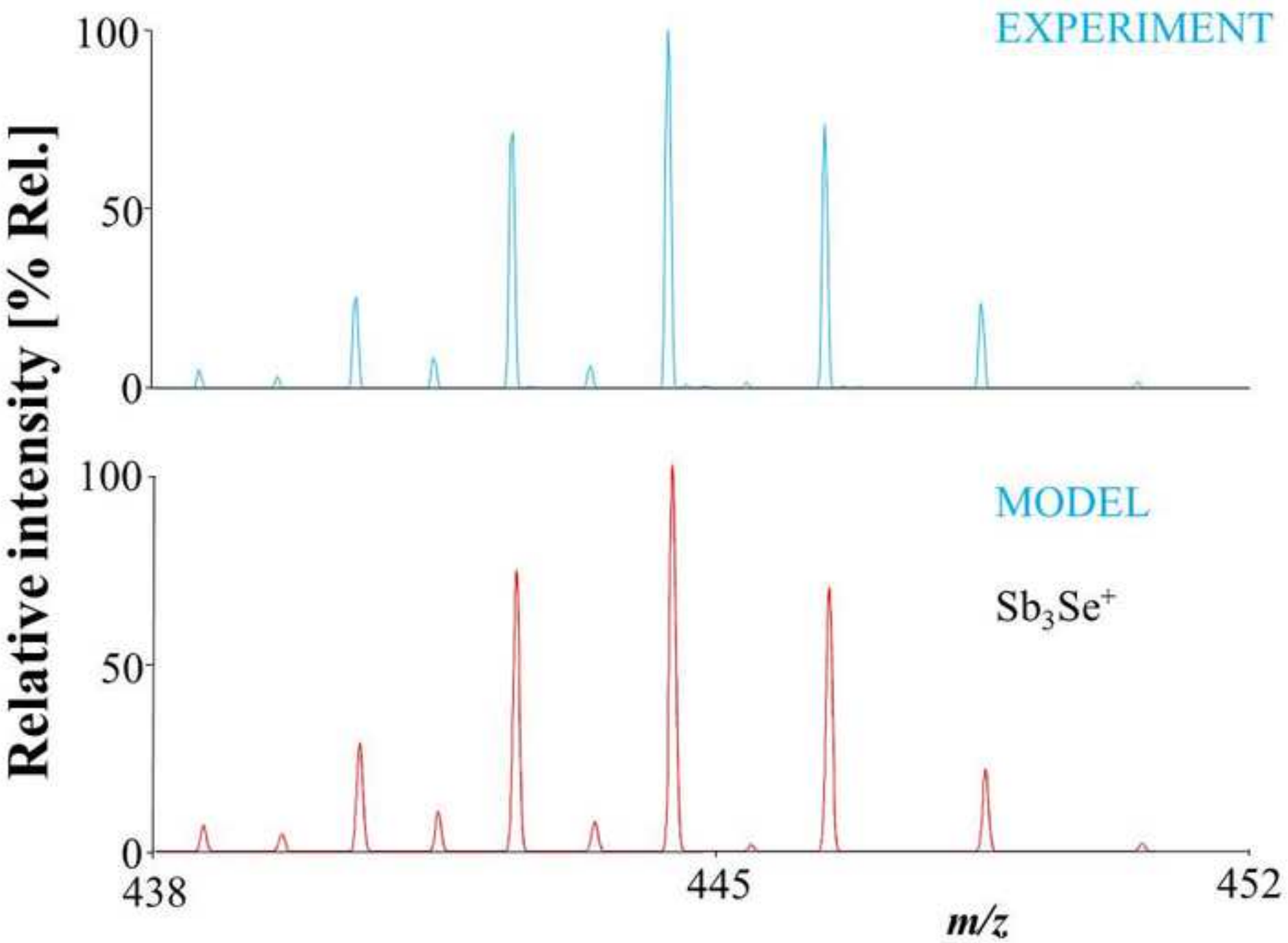

Figure S2A

Click here to access/download;Figures;Figure S2 A.jpg

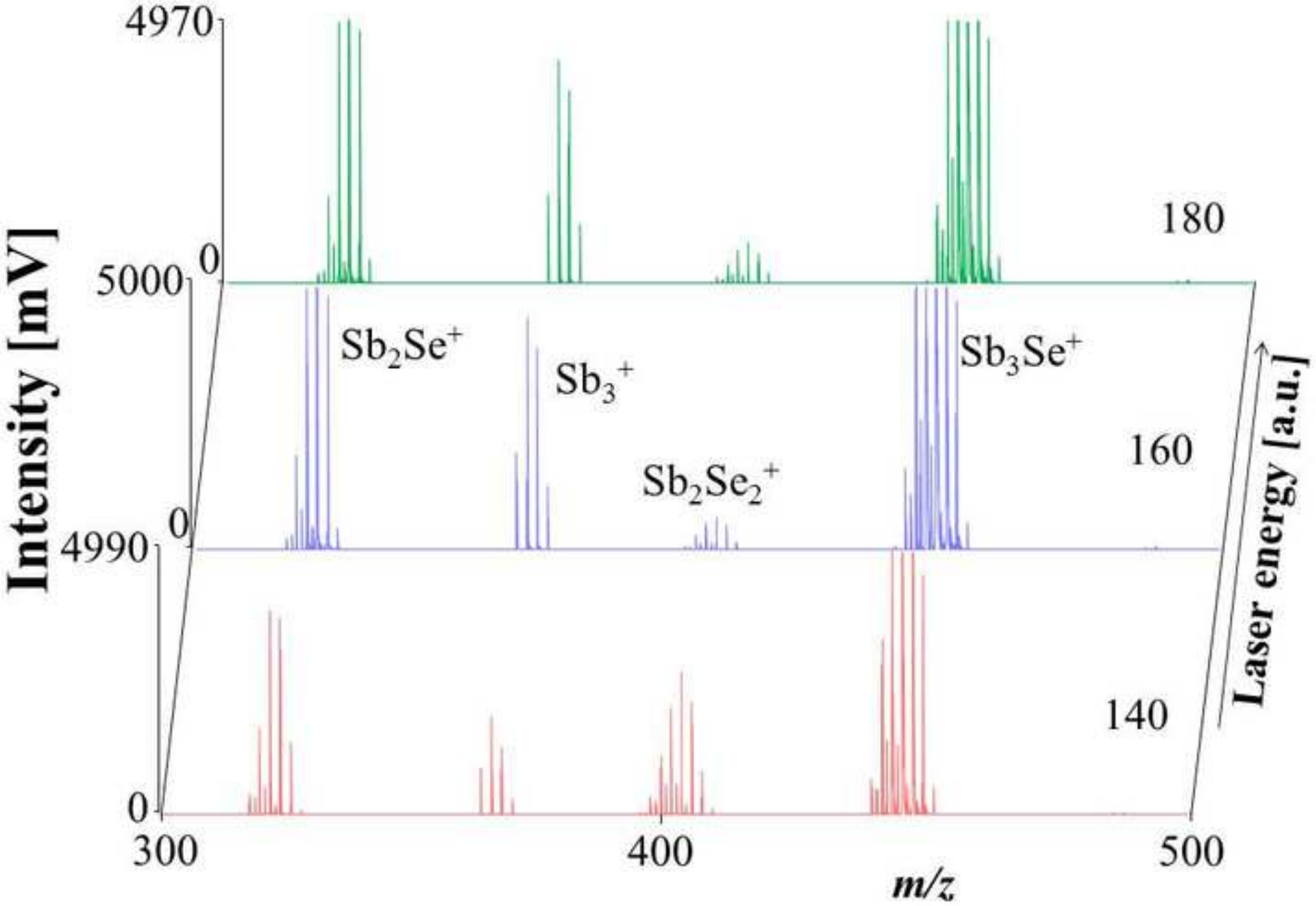

Figure S2B

Click here to access/download;Figures;Figure S2 B.jpg

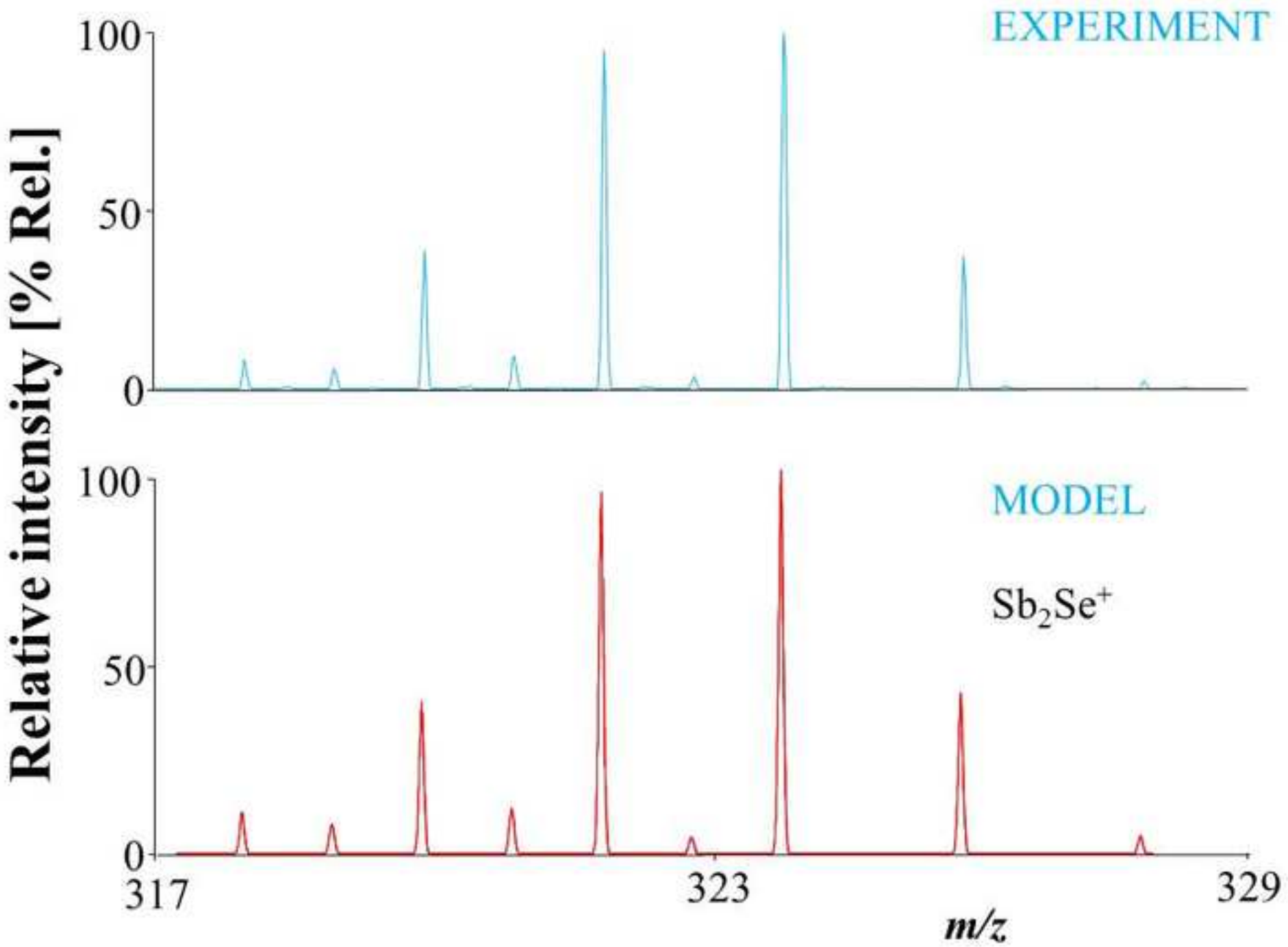

Figure S3A

Click here to access/download;Figures;Figure S3 A.jpg

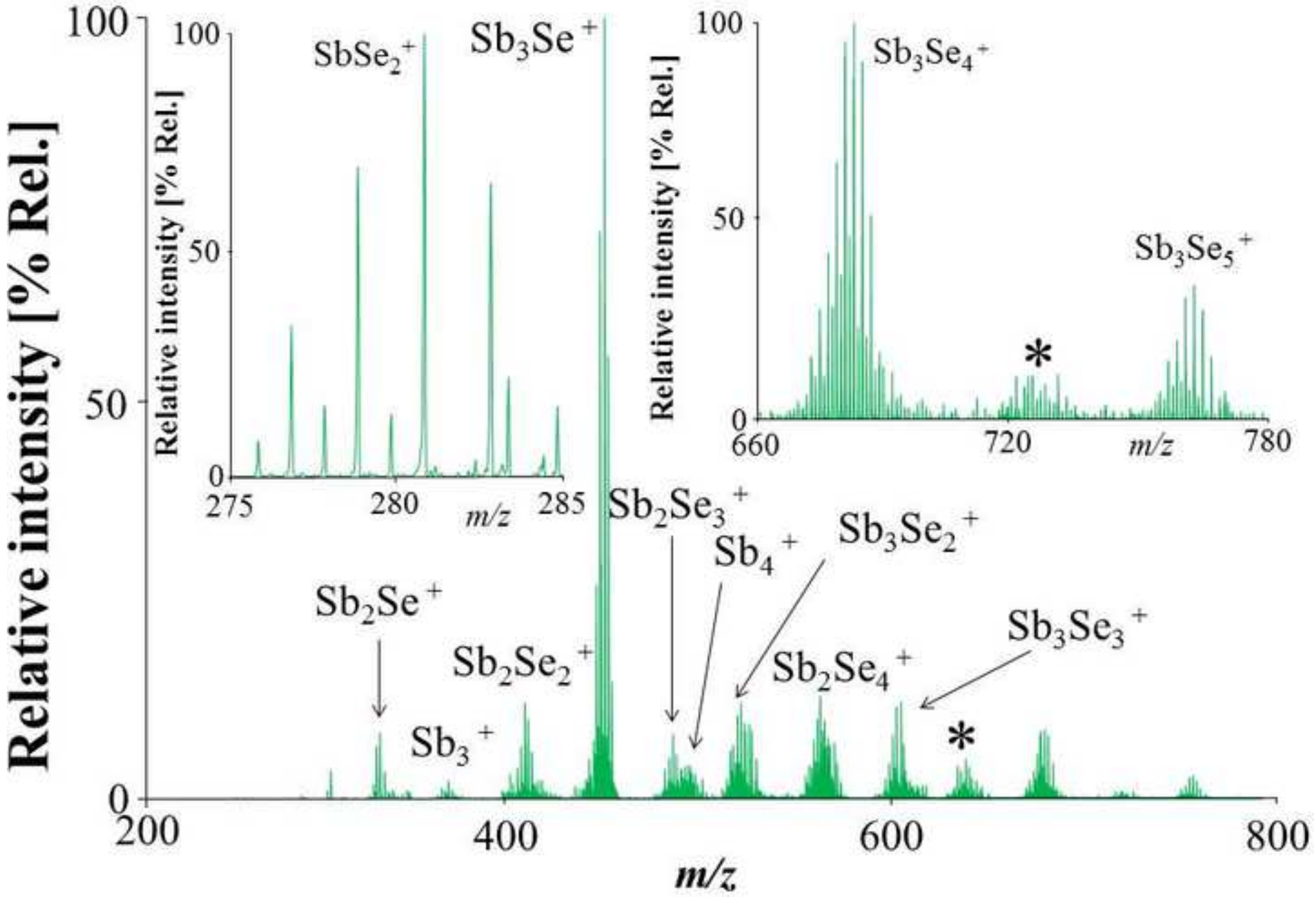

Figure S3B

Click here to access/download;Figures;Figure S3 B.jpg

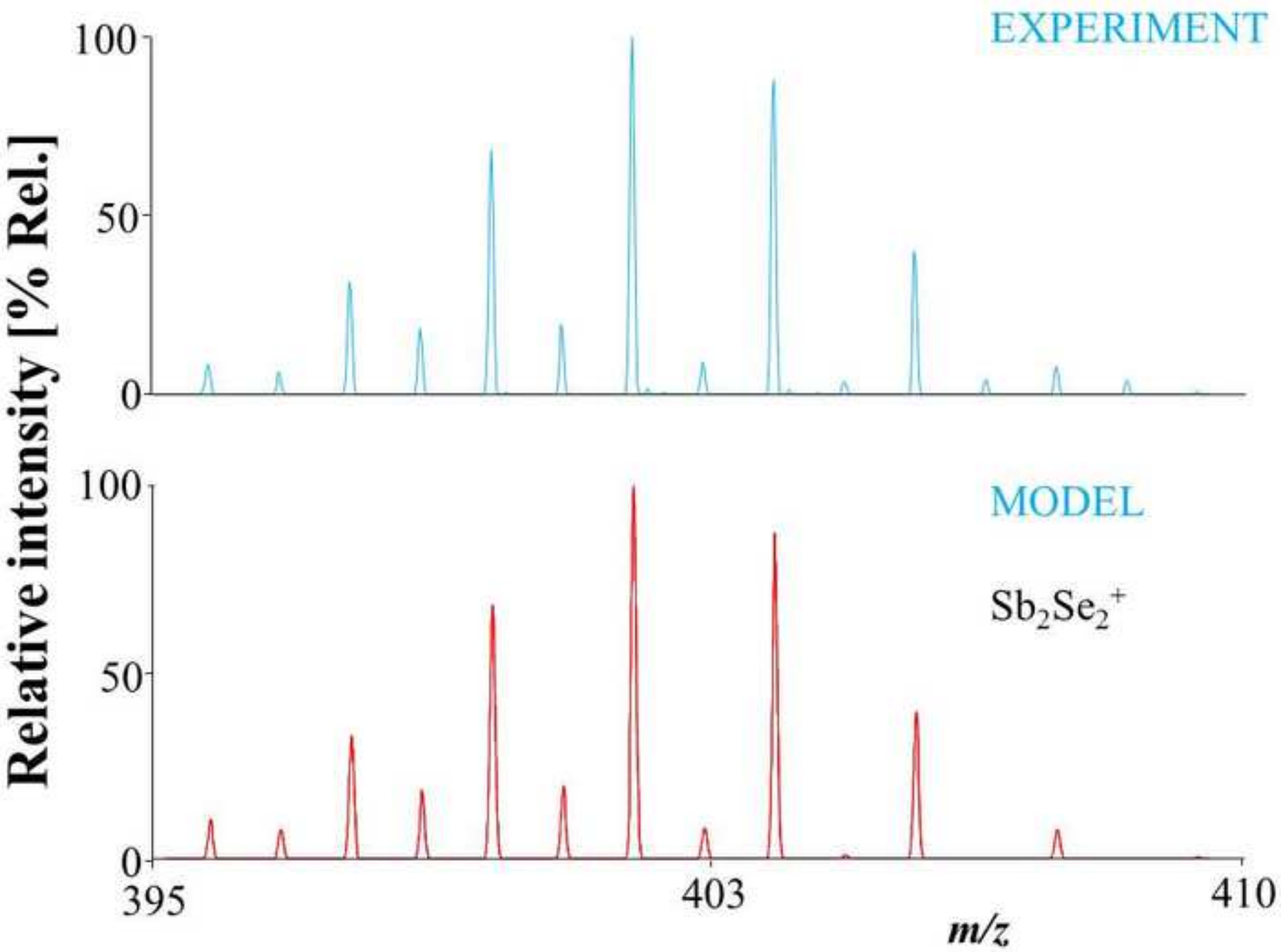

Figure S4

Click here to access/download;Figures;Figure S4.jpg

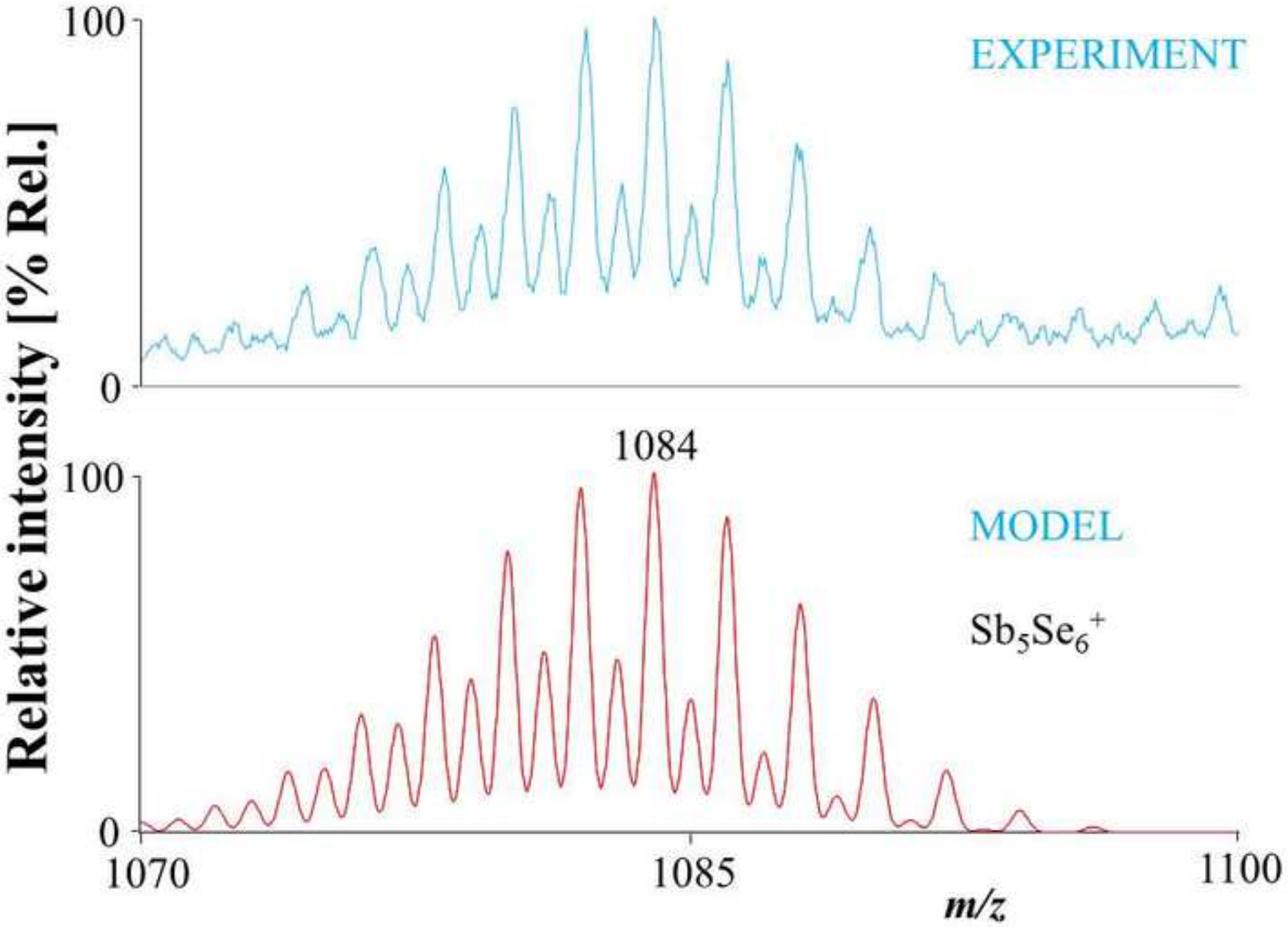

Figure S5A

Click here to access/download;Figures;Figure S5 A.jpg

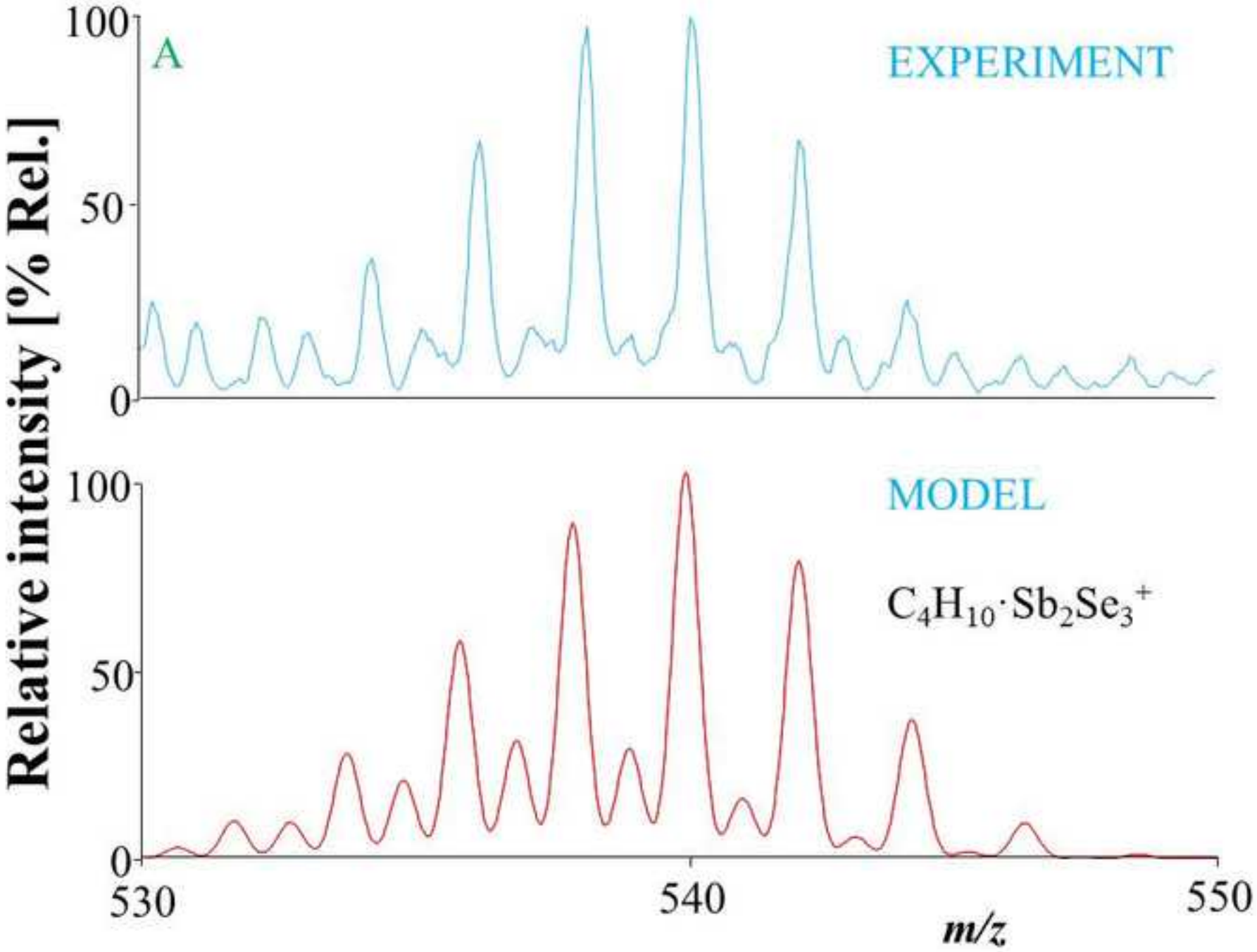

Figure S5B

Click here to access/download;Figures;Figure S5 B.jpg

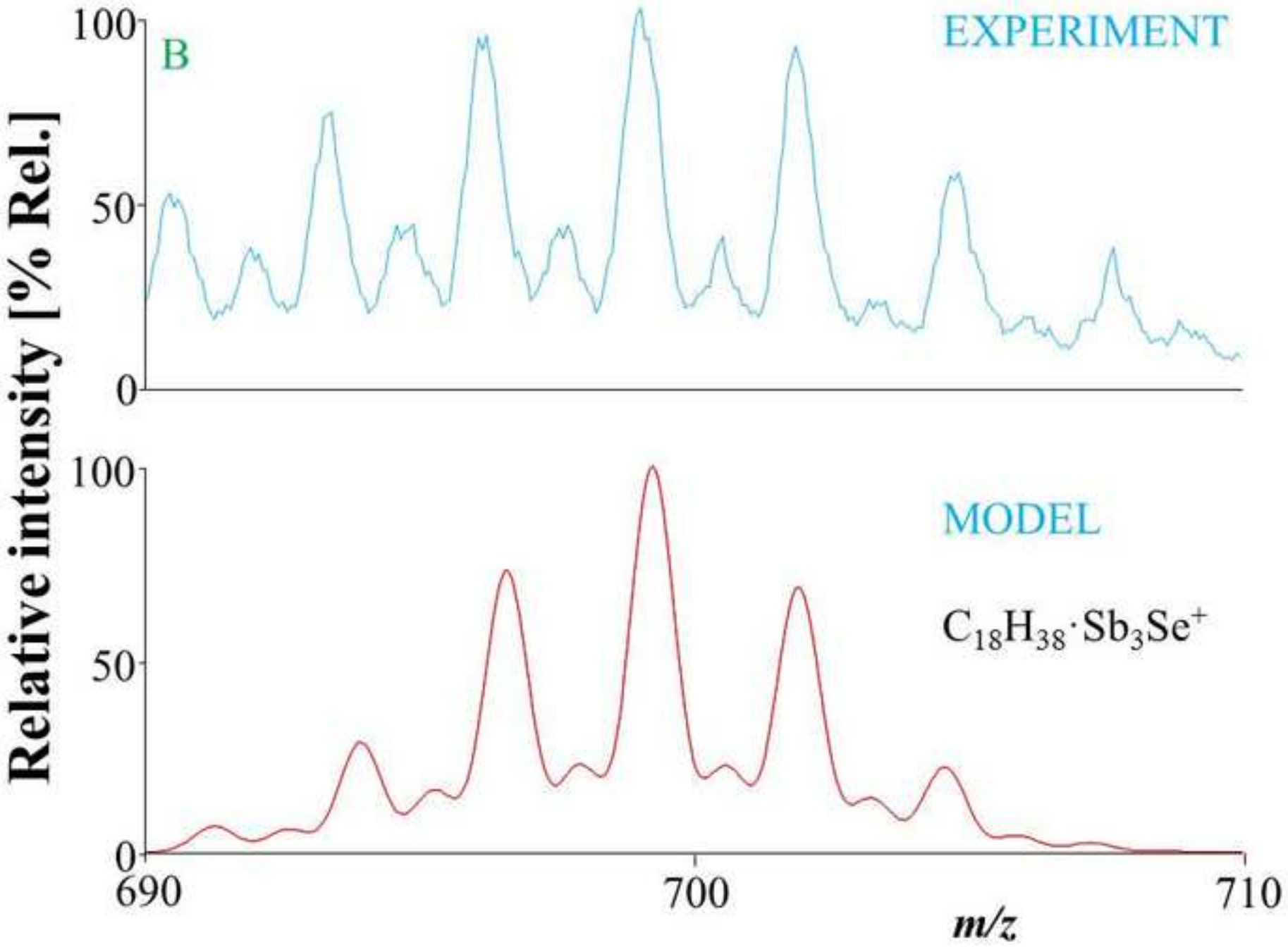

Graphical Abstract

Click here to access/download;Graphical Abstract;Graphical abstract.jpg

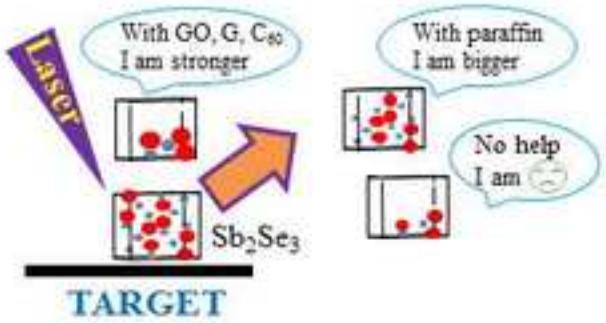

Click here to access/download
Supplemental Information
Supplement.docx